Molecular Therapy
Oncolytics
Original Article

Oncolytic Adenoviruses Armed with Tumor Necrosis Factor Alpha and Interleukin-2 Enable Successful Adoptive Cell Therapy

Riikka Havunen,[1] Mikko Siurala,[1,2] Suvi Sorsa,[1,2] Susanna Grönberg-Vähä-Koskela,[1] Michael Behr,[1,8] Siri Tähtinen,[1] João Manuel Santos,[1,2] Pauliina Karell,[3] Juuso Rusanen,[1] Dirk M. Nettelbeck,[4] Anja Ehrhardt,[5] Anna Kanerva,[1,6] and Akseli Hemminki[1,2,7]

[1]Cancer Gene Therapy Group, Faculty of Medicine, University of Helsinki, 00290 Helsinki, Finland; [2]TILT Biotherapeutics, Ltd., 00290 Helsinki, Finland; [3]Institute for Molecular Medicine Finland, University of Helsinki, 00290 Helsinki, Finland; [4]German Cancer Research Center (DKFZ), 69120 Heidelberg, Germany; [5]Faculty of Health, Institute for Virology and Microbiology, University Witten/Herdecke, 58448 Witten, Germany; [6]Department of Obstetrics and Gynecology, Helsinki University Central Hospital, 00610 Helsinki, Finland; [7]Comprehensive Cancer Center, Helsinki University Hospital, 00290 Helsinki, Finland

Adoptive cell therapy holds much promise in the treatment of cancer but results in solid tumors have been modest. The notable exception is tumor-infiltrating lymphocyte (TIL) therapy of melanoma, but this approach only works with high-dose preconditioning chemotherapy and systemic interleukin (IL)-2 postconditioning, both of which are associated with toxicities. To improve and broaden the applicability of adoptive cell transfer, we constructed oncolytic adenoviruses coding for human IL-2 (hIL2), tumor necrosis factor alpha (TNF-α), or both. The viruses showed potent antitumor efficacy against human tumors in immunocompromised severe combined immunodeficiency (SCID) mice. In immunocompetent Syrian hamsters, we combined the viruses with TIL transfer and were able to cure 100% of the animals. Cured animals were protected against tumor re-challenge, indicating a memory response. Arming with IL-2 and TNF-α increased the frequency of both $CD4^+$ and $CD8^+$ TILs in vivo and augmented splenocyte proliferation ex vivo, suggesting that the cytokines were important for T cell persistence and proliferation. Cytokine expression was limited to tumors and treatment-related signs of systemic toxicity were absent, suggesting safety. To conclude, cytokine-armed oncolytic adenoviruses enhanced adoptive cell therapy by favorable alteration of the tumor microenvironment. A clinical trial is in progress to study the utility of Ad5/3-E2F-d24-hTNFa-IRES-hIL2 (TILT-123) in human patients with cancer.

INTRODUCTION

Immunotherapies have shown promising results in cancer types previously hard to cure, such as melanoma,[1–3] non-small cell lung cancer,[4] and renal cell carcinoma.[5] In addition to checkpoint-inhibiting antibodies, patient-derived T cells are a potent approach because they can be re-targeted against tumors ex vivo, or they can be infused to the patient without modifications, when extracted from the tumor biopsy.[6] One advantage of using biopsy-derived polyclonal tumor-infiltrating lymphocytes (TILs) is the presence of neoantigen-specific clones—an aspect absent from receptor-modified T cells.[7] As a downside, TIL infusion requires high-dose preconditioning to eradicate suppressive immune cell subsets from the tumor microenvironment and postconditioning with high-dose systemic interleukin (IL)-2, both often causing severe toxicities.[6,8]

Instead of systemic administration of cytokines like IL-2, it could be more attractive to deliver them locally with gene therapy vectors, such as viruses.[9,10] In particular, tumor-targeted replication-competent viruses (i.e., oncolytic viruses) enable a thousand-fold amplification of transgene expression, restricted to tumor tissue. With regard to immunotherapy, oncolytic adenovirus constitutes a personalized cancer vaccine generated for each patient in situ, due to release of tumor-associated antigens.[11] Of note, virus-mediated danger signaling helps the immune system to recognize tumor cells,[12] and immunostimulatory cytokines further boost this effect.[3,13,14]

We have shown that the most promising T cell-stimulating factors, in the context of adoptive cell therapy, are IL-2 and tumor necrosis factor alpha (TNF-α).[15–17] Regarding prior knowledge about the recombinant proteins, IL-2 has been widely used in treating malignant melanoma and renal cell carcinoma[18] and it stimulates T cell proliferation and differentiation.[9,19,20] Like IL-2, TNF-α can activate immune cells,[21] but it also induces antitumor inflammation and the production of other cytokines and chemokines.[22,23] Moreover, it directly causes cancer cell necrosis and apoptosis.[23]

In this study, we constructed and characterized new oncolytic adenoviruses built on a backbone of Ad5/3-E2F-d24 (OAd) carrying human

Received 29 November 2016; accepted 20 December 2016;
http://dx.doi.org/10.1016/j.omto.2016.12.004.

[8]Present address: IPM Biotech, GmbH, Lademannbogen 10, 22339 Hamburg, Germany

Correspondence: Akseli Hemminki, Cancer Gene Therapy Group, Faculty of Medicine, University of Helsinki, Haartmaninkatu 3, 00290 Helsinki, Finland.
E-mail: akseli.hemminki@helsinki.fi

This is an open access article under the CC BY-NC-ND license (http://creativecommons.org/licenses/by-nc-nd/4.0/).

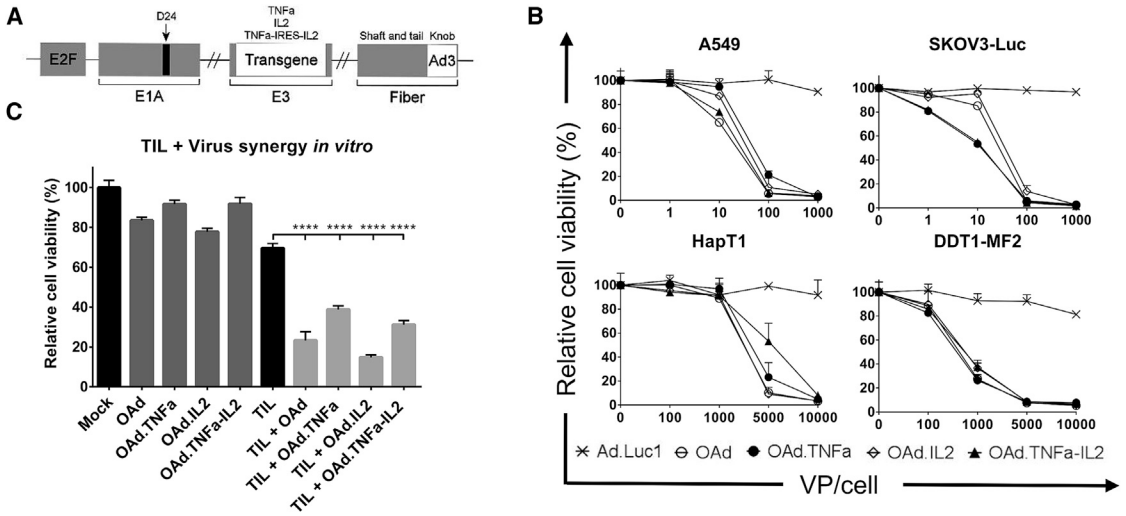

Figure 1. Oncolytic Activity of Adenoviral Vectors in Human and Hamster Cancer Cell Lines

(A) A schematic presentation of chimeric oncolytic adenovirus with E2F promoter; 24-base-pair deletion in *E1A*; human TNF-α, IL-2, or TNF-α-IRES-IL2 inserted in the *E3* region; and an Ad3 serotype knob in the Ad5 fiber. (B) Oncolytic activity of the viruses was shown in human lung adenocarcinoma (A549) and luciferase-expressing ovarian carcinoma (SKOV3-Luc) as well as in hamster pancreatic cancer (HapT1) and leiomyosarcoma (DDT1-MF2). The cells were incubated with the viruses for 3 days (A549 and DDT1-MF2), 5 days (SKOV3-Luc), or 6 days (HapT1) before determining cell viability. (C) Cell-killing efficacy was enhanced when combining viruses with HapT1-specific TILs. The cells were incubated 72 hr with 5,000 VPs and 24 hr with TILs. Means ± SEM are shown (n = 8). Statistical differences were evaluated with one-way ANOVA. ****$p \leq 0.0001$. Ad.Luc1, replication-deficient Ad5/3-Luc1; OAd, Ad5/3-E2F-d24; OAd.TNFa, Ad5/3-E2F-d24-hTNFa; OAd.IL2, Ad5/3-E2F-d24-hIL2; OAd.TNFa-IL2, Ad5/3-E2F-d24-hTNFa-IRES-hIL2.

IL-2 (hIL2), TNF-α, or both. Two modifications render virus replication tumor specific: an E2F promoter and a 24-base pair (bp) deletion in the constant region 2 of *E1A*, make the viruses selective for cells defective in the retinoblastoma/p16 pathway—including most tumor cells.[24,25] In addition, the Ad5/3 chimeric capsid featuring the Ad3 knob but Ad5 shaft and tail has demonstrated improved cancer cell transduction as well as antitumor efficacy.[26] Importantly, safety of this configuration in humans has also been established.[13,27,28] Based on the results in an immunocompetent Syrian hamster model of pancreatic cancer, these viruses emerged as strong candidates for stimulating the immune system in tumors locally, with the specific application of enabling effective and safe TIL therapy. Ad5/3-E2F-d24-hTNFa-IRES-hIL2 (TILT-123) rose as the leading candidate for human translation.

RESULTS

Armed Oncolytic Adenoviruses Have Cell-Killing Ability, Show Synergy When Combined with TILs, and Express Biologically Active Cytokines

Oncolytic adenoviruses were constructed to feature a backbone carrying serotype 5 (Ad5) nucleic acid with an Ad3 fiber knob. In addition, a 24-bp deletion (d24) in the Rb-binding region of adenoviral *E1A* together with the E2F promoter was established to direct the replication to Rb-deficient cancer cells. The transgenes were inserted into the *E3* region, to replace some superfluous adenoviral open reading frames, which links expression to virus replication (Figure 1A).

All cytokine-armed adenovirus constructs were able to kill a panel of human cancer cell lines with similar efficacy as the virus without transgenes (Figures 1B and S1). Importantly, when virus was combined with HapT1-targeting TILs, the cell-killing effect was significantly increased (Figure 1C). Both human and hamster cells were able to produce biologically active human IL-2 as well as TNF-α in vitro when infected with armed viruses (Figures 2A, 2B, and S2). Importantly, local production of cytokines was observed with all three armed viruses in vivo while systemic levels remained undetectable (Figure 2C), highlighting the feasibility of the technology from a safety perspective.

Cytokine-Armed Viruses Inhibit Tumor Growth in a Dose-Dependent Manner

To establish an optimal virus dose, immunocompromised mice bearing orthotopic human ovarian tumors (SKOV3-Luc) received three different doses of Ad5/3-E2F-d24-hTNFa-IRES-hIL2. The best efficacy was achieved with the highest dose of 1×10^9 viral particles (VPs), which was significantly different compared with the untreated control group ($p = 0.0085$) as well as with the lowest dose of 1×10^5 VPs ($p = 0.0287$) on day 18 (Figure 3A). When SKOV3-Luc tumors were treated with Ad5/3-E2F-d24-hTNFa-IRES-hIL2 and control viruses, all viruses had similar antitumor efficacy (Figures 3B and 3C), suggesting that adenovirus replication rates in vivo were comparable despite the inclusion of transgenes.

Armed Oncolytic Viruses Improve the Efficacy of Adoptive TIL Transfer

Encouraged by the ex vivo results (Figure 1C), the ability of cytokine-armed viruses to enhance TIL therapy was investigated in immunocompetent Syrian hamsters (Figure 4). The unarmed virus and TILs

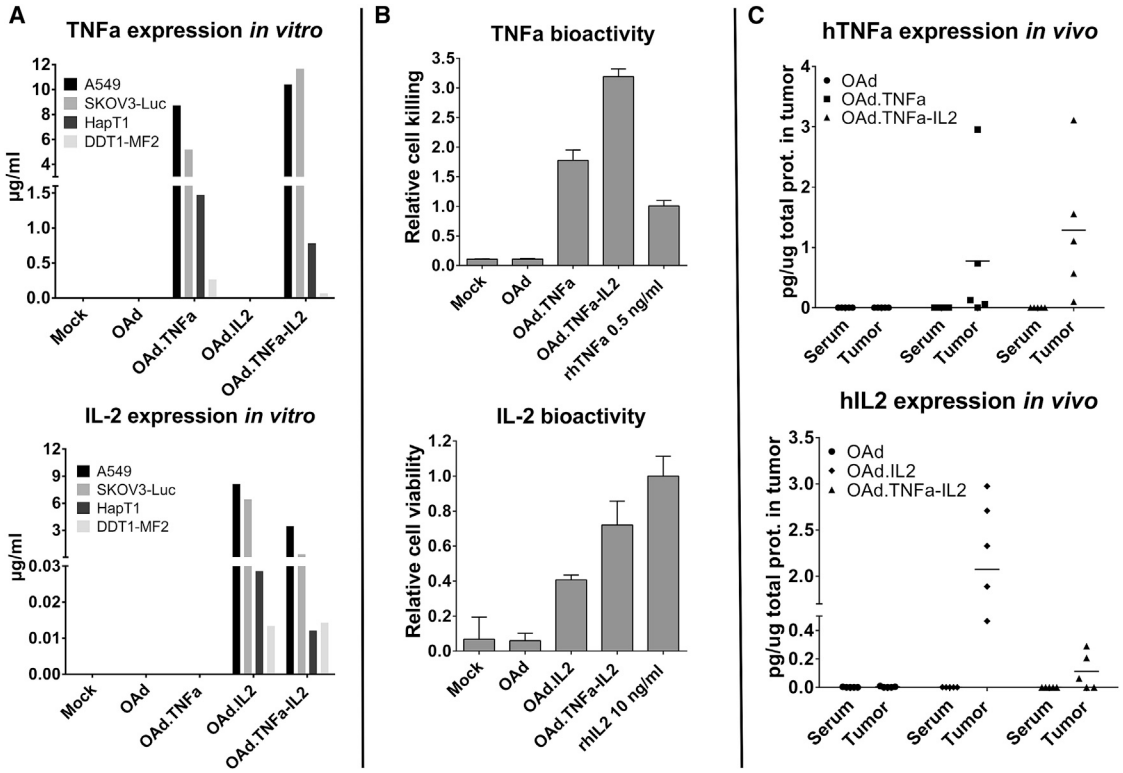

Figure 2. Biologically Active Cytokines Are Produced from Human and Hamster Cell Lines and Expressed Locally In Vivo

(A) Human and hamster cell lines were incubated for 72 hr with 1,000 or 5,000 VPs per cell, respectively. Cytokine concentrations were measured from cell culture supernatants with a cytometric bead array. (B) Indicator cell line L929 was used in the cell-killing assay to confirm the biological activity of TNF-α, while mouse T cell line CTLL-2 was utilized in the IL-2-induced cell proliferation assay. The samples were derived from virus-infected HapT1 supernatants. Means ± SD are shown. (C) HapT1 tumors were injected with 1×10^8 VPs and collected together with blood after 48 hr. Cytokine concentrations were measured with a cytometric bead array and normalized against total protein concentration of the sample. Horizontal lines indicate mean values. OAd, Ad5/3-E2F-d24; OAd.TNFa, Ad5/3-E2F-d24-hTNFa; OAd.IL2, Ad5/3-E2F-d24-hIL2; OAd.TNFa-IL2, Ad5/3-E2F-d24-hTNFa-IRES-hIL2.

had only moderate antitumor effects when administered alone, but a significant improvement in efficacy was observed when they were combined (p = 0.002) (Figure 4A). The armed viruses had tremendous efficacy even as single agents (Figures 4B–4D), but the percentage of cured animals was higher in groups receiving TILs and virus compared with the virus-only groups (p = 0.034; Figure 4E). In fact, cured hamsters treated with the combination of Ad5/3-E2F-d24-hTNFa-IRES-hIL2 and TIL therapy comprised 100% (Figure 4E). The experiment was repeated with a reduced virus dose with similar results in efficacy (Figure 4F). The cured animals from the second experiment stayed tumor free for the follow-up period of 3 months.

Cytokines Increase the Frequency of T Cells in Tumors and Augment Splenocyte Proliferation

To investigate immunological effects of the armed viruses, cells from tumors, spleens, and tumor-draining lymph nodes were analyzed with flow cytometry (Figures 5A–5E and S3). Natural killer (NK) cell marker GM1 and T cell markers CD8 and CD4 were more frequent in tumors treated with IL-2, whereas the cytokine combination was the only treatment capable of increasing the level of major histocompatibility complex class II (MHC II) and decreasing the Mac-2 expression in tumors (Figures 5A–5E). Differences in the cell composition in spleens and lymph nodes were minor (Figure S3). Interestingly, splenocytes exhibited greater cell proliferation ex vivo if the animals had been treated with armed viruses (Figure 5F).

Treatments with Cytokine-Armed Viruses Induce Protection from Tumor Re-challenge

To estimate whether the viral treatment established tumor-specific immunity, cured hamsters were re-challenged with the same cancer cells as previously (HapT1). As a control, different types of cancer cells (DDT1-MF2) were implanted in the other flank of the animal (Figure 6). The animals that had previously been cured with cytokine-coding viruses rejected HapT1, whereas the animal treated with unarmed virus had a stable condition. The number of animals in these groups differs, because the curative potential of the unarmed virus was more limited. DDT1-MF2 tumor growth in cured hamsters was comparable to growth in naive

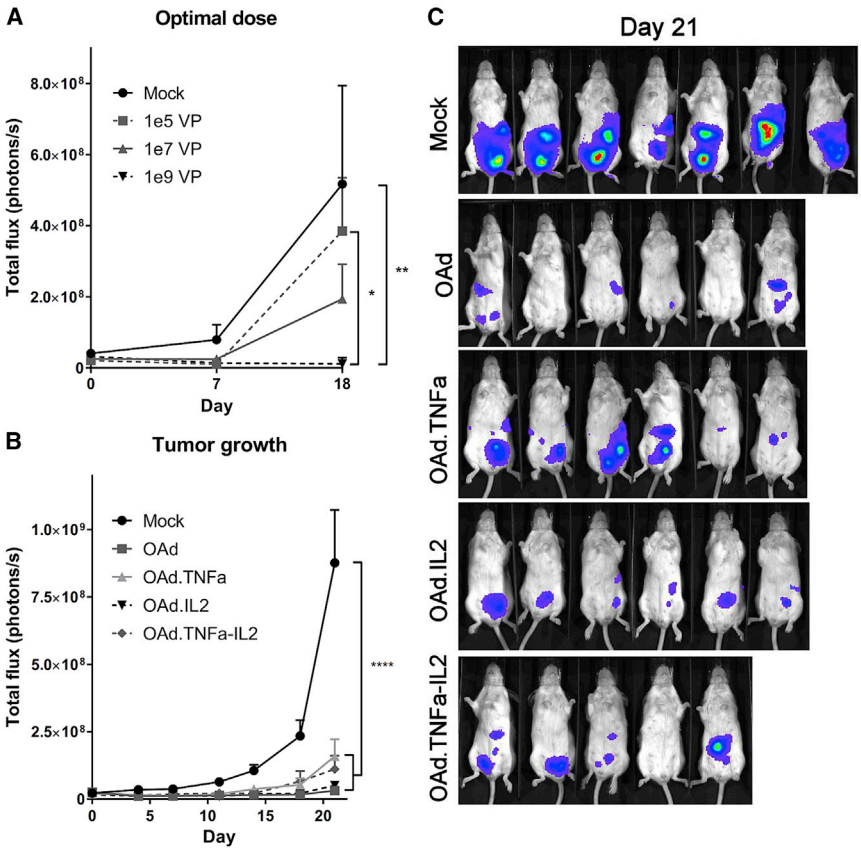

Figure 3. Armed Oncolytic Adenoviruses Show Dose-Dependent Antitumor Efficacy in Immunocompromised Mice

(A–C) SCID mice bearing orthotopic luciferase-expressing ovarian carcinoma SKOV3-Luc were treated with (A) different doses of Ad5/3-E2F-d24-hTNFa-IRES-hIL2 (n = 3) and with (B and C) all the viruses with selected dose (1×10^9 VPs/animal, n = 5–7). Means ± SEM are shown. Statistical differences were evaluated with two-way ANOVA. *$p \leq 0.05$; **$p \leq 0.01$; ****$p \leq 0.0001$. (C) Bioluminescent images from day 21 were merged with photographs. The color scale from violet to red represents luminescence intensity from 1×10^6 to 1×10^8 p/s/cm^2/sr, respectively. OAd, Ad5/3-E2F-d24; OAd.TNFa, Ad5/3-E2F-d24-hTNFa; OAd.IL2, Ad5/3-E2F-d24-hIL2; OAd.TNFa-IL2, Ad5/3-E2F-d24-hTNFa-IRES-hIL2.

animals, indicating the induction of tumor-specific antitumor immunity.

Virus Treatment Does Not Induce Major Histological Changes in Selected Organs

Treatment-related changes in tissue structures of the heart, lung, liver, and kidney were undetectable (Supplemental Materials and Methods). Meanwhile, spleens collected from all treatment groups showed mild and minimal lymphocyte hyperplasia, slightly expanded white pulp, and a mildly increased number of heterophils in the marginal zone or red pulp. There were no differences in the severity of the changes between any of the treatment groups including mock and other controls, suggesting a lack of systemic effects linked to the transgenes as predicted by low serum concentrations (Figure 2C).

DISCUSSION

Immuno-oncology has made some clinical breakthroughs over the years, but, currently, a minority of patients respond and single-agent treatment modalities seldom lead to lasting remissions.[1–4] Thus, the utility of immunotherapy has been established on a proof-of-concept level, but much work remains to help the majority of patients with currently incurable cancer. Checkpoint-inhibiting antibodies have received much attention due to their ability to downregulate immunosuppression, but they cannot generate new immunity.[29] By contrast, new immune reactions can be achieved with adoptive cell therapies and oncolytic immunotherapy, thus being complementary to the former.[29] However, adoptive cell therapy of non-melanoma solid tumors has proved clinically unimpressive results, because the tumor microenvironment is able to anergize the cell graft.[16,30] This effect can be countered with the biological phenomena resulting from adenoviral oncolysis, and it can be optimized with TNF-α and IL-2.[16,31] We previously studied the effects of these cytokines with recombinant cytokines and with replication-defective vectors coding for murine cytokines.[15–17] Here, we constructed clinically applicable oncolytic adenoviruses coding for human IL-2 and TNF-α and used them to boost adoptive cell transfer.

The viruses were capable of infecting and lysing a variety of human and Syrian hamster cancer cell lines. In addition, infected cells produced bioactive cytokines. After intratumoral virus administration, high cytokine concentrations were achieved in target tissue, while blood levels remained undetectable. In addition, signs of toxicity were absent in histopathological evaluation of all major organs. Taking into consideration the potential toxicity of high systemic cytokine levels,[8,32] the results suggest a safer approach for cytokine delivery. Moreover, local delivery of IL-2 could replace the need for high-dose IL-2 administration often included in clinical T cell therapy protocols,[6] although detailed studies are needed to validate the concept.

To investigate the efficacy of the viruses on human cancer cells in vivo, we established an orthotopic ovarian carcinoma model in immunocompromised SCID mice. Despite the replication competence of the virus, the efficacy was dose dependent. The problem of virus infiltration into the tumor is well known; thus, intratumoral administration represents a more efficient way of delivering the virus.[33] In addition, this model develops resistance to oncolytic adenovirus, seen as a reduction in antitumor efficacy at later time points. The mechanism

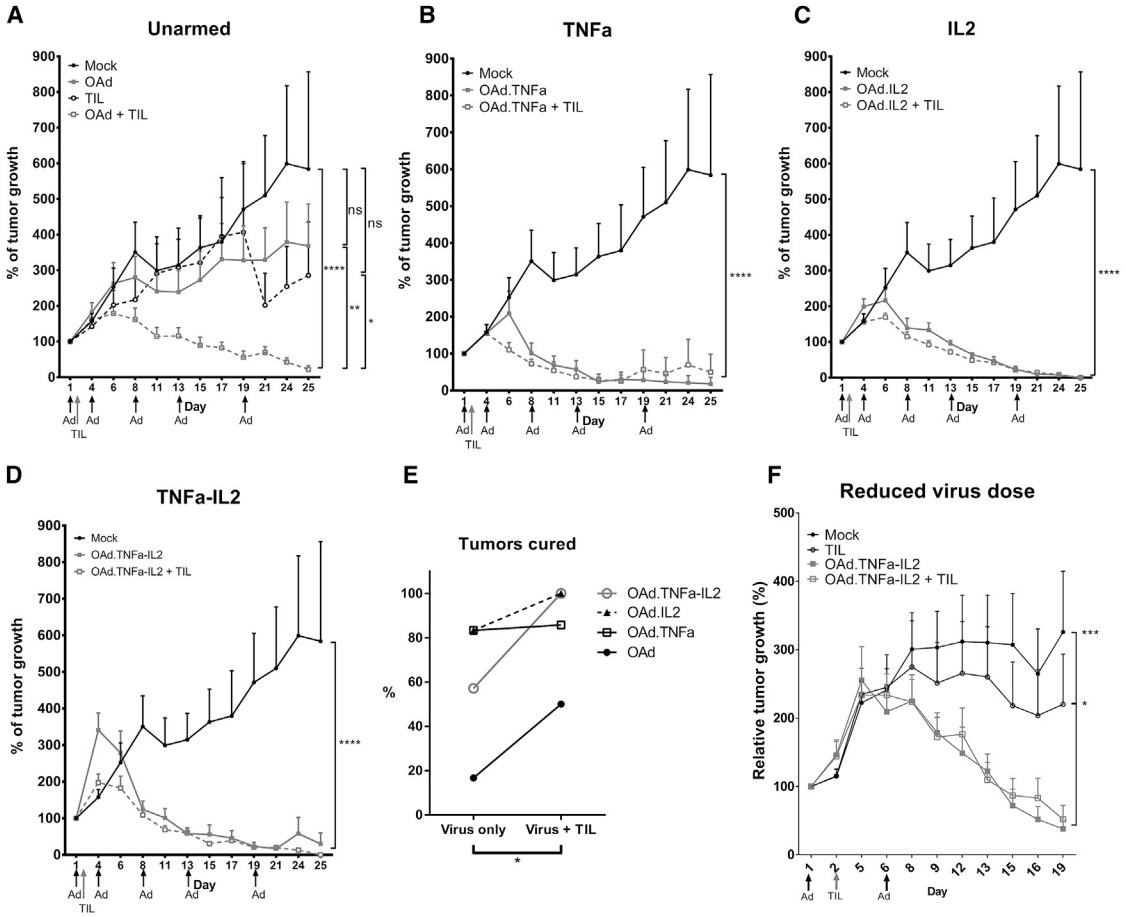

Figure 4. Armed Oncolytic Adenoviruses Improve the Curative Efficacy of Adoptive TIL Therapy in Immunocompetent Syrian Hamsters

(A–D) Syrian hamsters with established subcutaneous HapT1 tumors were treated five times with 1×10^9 VPs and once with 4×10^5 freshly expanded TILs, both injected intratumorally (n = 6–7). Tumors lacking neoplastic cells were considered cured. Statistical differences were evaluated with a linear mixed-effects model. (E) Complete tumor remission was evaluated before animals were euthanized or in unclear cases after histopathological analysis. The effect of TILs on cure rates was evaluated with the Wilcoxon signed-rank test. (F) The experiment was repeated with a reduced virus dose (1×10^8 VPs on days 1 and 8, n = 5–6). Differences in antitumor efficacy were analyzed with two-way ANOVA. *$p \leq 0.05$; **$p \leq 0.01$; ***$p \leq 0.001$; ****$p \leq 0.0001$. ns, non-significant; OAd, Ad5/3-E2F-d24; OAd.TNFa, Ad5/3-E2F-d24-hTNFa; OAd.IL2, Ad5/3-E2F-d24-hIL2; OAd.TNFa-IL2, Ad5/3-E2F-d24-hTNFa-IRES-hIL2.

of resistance was previously shown to be related to the induction of interferon pathways.[34] Significant differences in the efficacy between the viruses were absent, which was expected because the cytokines have few effects in an immunocompromised model lacking a complete immune system.

Cytokine-armed oncolytic viruses are potential enhancers of T cells and T cell-based therapies.[14,35,36] To investigate the synergy between our viruses and TILs, we chose Syrian hamsters as an immunocompetent animal model. Syrian hamsters provide an interesting model for studying oncolytic adenoviruses, since human adenovirus is capable of replicating in hamsters, unlike in mice.[37] Conveniently, human IL-2[38] and human TNF-α are also bioactive in hamsters, which is evident from the hamster experiment where the unarmed virus had only moderate antitumor effects as compared with the human cytokine-coding viruses that share the same backbone construct. Furthermore, we have developed a method to extract and expand TILs from established hamster tumors, despite the limited availability of hamster-specific reagents.[39] Unfortunately, specific expansion of, for example, $CD8^+$ T cells is unfeasible and the TIL pool depends on the population present in the tumor at the time of collection.

Even in vitro, the synergistic effect of combining the viruses and TILs was evident. In vivo, the combination of unarmed virus and TILs led to improvement in efficacy. With regard to the cytokine-armed viruses, good efficacy was seen with single-agent treatment in two individual experiments. However, the combination of armed virus and TIL therapy resulted in the highest frequency of complete responses, as confirmed by histopathological analysis of the tumors. Of note, all tumors in hamsters treated with Ad5/3-E2F-d24-hTNFa-IRES-hIL2 and TILs were cured, suggesting that inclusion of adenovirally

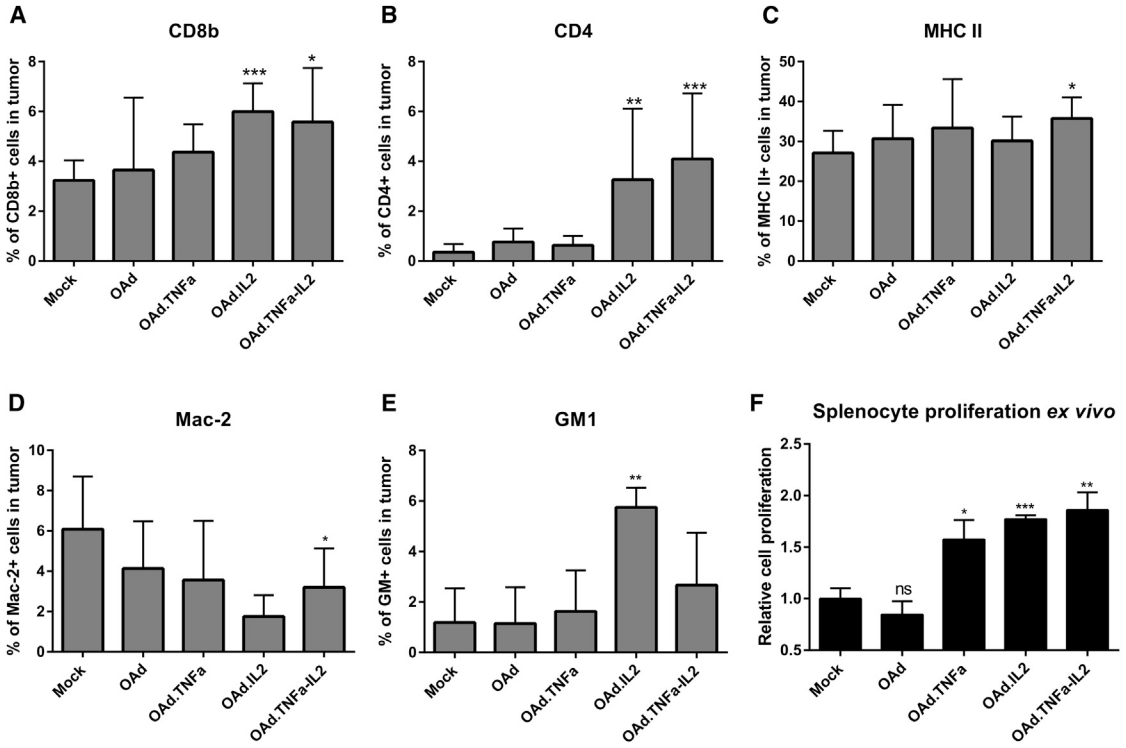

Figure 5. Adenovirus Treatments Induce Beneficial Immunological Changes in Tumor Microenvironment

(A–E) The following cells were stained from endpoint tumors with fluorochrome-conjugated antibodies and analyzed by flow cytometry: (A) $CD8^+$, (B) $CD4^+$, (C) MHC II^+, (D) Mac-2^+, and (E) $GM1^+$. Because of the great number of cured tumors, groups with or without TILs were combined. Means ± SD are shown (n = 3–9). Differences in cell percentages were analyzed with the Student's t test. (F) Splenocyte proliferation was determined by counting the cells. Because TILs did not affect the proliferation, groups with or without TILs were combined for simplification. Means ± SEM are shown (n = 4). Statistical significance was calculated with the non-parametric Mann-Whitney test. *$p \leq 0.05$; **$p \leq 0.01$; ***$p \leq 0.001$. ns, non-significant; OAd, Ad5/3-E2F-d24; OAd.TNFa, Ad5/3-E2F-d24-hTNFa; OAd.IL2, Ad5/3-E2F-d24-hIL2; OAd.TNFa-IL2, Ad5/3-E2F-d24-hTNFa-IRES-hIL2.

delivered immunostimulatory cytokines contributes to the curative efficacy of TIL therapy.

Immunocompetent mouse models have revealed that combining adenovirus-delivered TNF-α and IL-2 with adoptive T cell transfer decreases immunosuppressive characteristics of the tumor microenvironment and increases the number of active cytotoxic T cells in melanoma tumors.[15,17] Moreover, mouse studies have revealed that the danger signals and immunostimulation caused by adenovirus and cytokines can result in repertoire expansion by polyclonal amplification of many classes of antitumor T cells while T cell exhaustion seems to be thwarted.[15–17]

Mouse tumor models are useful for immunological studies because many reagents are available. However, human adenovirus does not replicate productively in mouse tissues; therefore, the hamster model has some advantages in this regard. Unfortunately, the repertoire of reagents available for hamster studies is much more limited. There are only a few hamster-specific or cross-reactive antibodies, and only limited characterization of the immune cell subsets in the tumor is possible.

Nevertheless, we saw decreased presence of macrophage marker Mac-2 in the hamster tumors, whereas the frequency of $GM1^+$ (mostly NK) cells as well as $CD4^+$ and $CD8^+$ T cells was increased following intratumoral treatment with the cytokine-coding viruses. Balza et al.[31] observed from immunocompetent mice that both $CD8^+$ and $CD4^+$ cells are essential for antitumor efficacy resulting from the combination of TNF-α and IL-2. IL-2 induces both regulatory and helper T cells;[40] however, in this study, the nature of $CD4^+$ cells could not be specified. Interestingly, the observed upregulation of MHC II (a marker for antigen-presenting cells) might indicate that the combination of both cytokines enables efficient tumor recognition by cytotoxic $CD4^+$ T cells,[39,41] thus contributing to the overall efficacy. In addition, the presence of TNF-α stimulates the expression of IL-6, a cytokine needed for helper T cell differentiation.[40,42] Taken together, although systemic IL-2 may cause stimulation of regulatory T cells, which may not necessarily be true for local IL-2, the possibility of the $CD4^+$ population also containing cytotoxic and helper T cells cannot be excluded.

In addition to immunological changes seen in the tumor microenvironment, further benefit from the cytokines was seen on the systemic

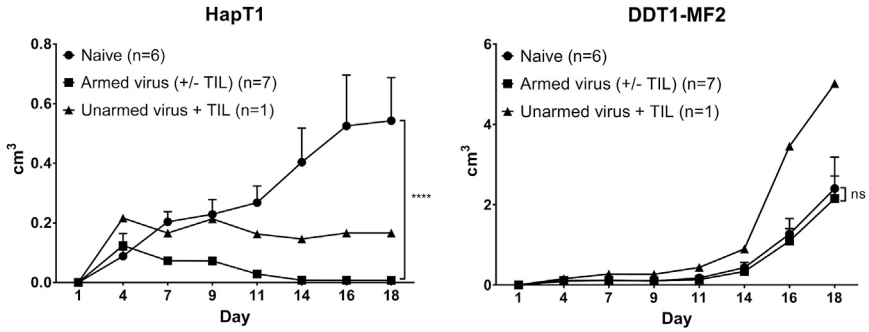

Figure 6. Cytokine-Armed Virus Treatments Induce Tumor-Specific Immunological Memory

Hamsters previously cured of HapT1 tumors were re-challenged with the same HapT1 tumor cells or with a distinct cell line (DDT1-MF2). Hamsters previously treated with cytokine-armed viruses completely rejected the re-introduced HapT1 tumors, whereas the hamster treated with unarmed virus had a stable condition. Means ± SEM are presented. ****$p \leq 0.0001$. ns, non-significant.

level. Because the spleen serves as an indicator for the common status of the immune system, we investigated the proliferative capability of the splenocytes derived from the treated animals ex vivo. Interestingly, the splenocytes from the cytokine-treated animals showed increased proliferative capability compared with the controls, indicating increased adaptive cellular response. The same effect has been seen in a study with oncolytic vaccinia virus coding for granulocyte-macrophage colony-stimulating factor.[10] Moreover, adenovirally encoded cytokines evidently induced the formation of immunological memory, typically mediated by T cells.[43] Currently, because there are no anti-hamster antibodies available, the presence of memory-type T cells could not be verified. The animals treated with armed viruses resisted tumor recurrence unlike the animal treated with the virus without the cytokines, as also seen with other oncolytic viruses.[10,43,44]

In conclusion, we provide evidence that oncolytic adenoviruses coding for human IL-2 and TNF-α appear safe in immunocompetent hamsters. In addition to direct oncolytic effects and attractive immunological effects, these viruses seem useful for enabling successful TIL therapy of human solid tumors. Whereas the virus itself shows potent antitumor efficacy, the cytokines are useful for induction of T cells in the tumor and for immunological memory responses. The preclinical data reported here allowed TILT Biotherapeutics to initiate a human trial studying the utility of Ad5/3-E2F-d24-TNFa-IRES-hIL2 in patients with advanced cancer receiving TIL therapy.

MATERIALS AND METHODS

Cell Lines

All cell lines were purchased from American Type Culture Collection (ATCC) unless otherwise stated. Human lung adenocarcinoma A549, human pancreatic cancer Panc1, human melanoma SK-MEL-28, human ovarian carcinoma OVCAR-3, mouse fibroblast L929, and mouse T lymphocyte cell line CTLL-2 were utilized in in vitro assays. Firefly luciferase-expressing ovarian adenocarcinoma SKOV3-Luc (kindly provided by Dr. Negrin, Stanford Medical School), hamster leiomyosarcoma DDT1-MF2 (a kind gift from Dr. William Wold), and hamster pancreatic cancer HapT1 (DSMZ) were used both in vitro and in vivo. All cell lines were maintained in RPMI 1640 or DMEM supplemented with 10% fetal bovine serum (FBS), 2 mM L-glutamine, 100 U/mL penicillin, and 100 μg/mL streptomycin (all from Sigma-Aldrich) and cultured at +37°C and 5% CO_2.

Generation of Viral Constructs

The experimental viruses have a backbone of Ad5/3-E2F-d24. The transgenes in Ad5/3-E2F-d24-hIL2 (OAd.IL2), Ad5/3-E2F-d24-hTNFa (OAd.TNFa), and Ad5/3-E2F-d24-hTNFa-IRES-hIL2 (OAd.TNFa-IL2, also known as TILT-123) were placed into the *E3* region and they were generated with the bacterial artificial chromosome (BAC)-recombineering strategy based on the selection marker galK adapted from Warming et al.,[45] Ruzsics et al.,[46] and Mück-Häusl et al.[47]

Plasmids were propagated in ElectroMAX DH5α-E Competent Cells (Thermo Fisher Scientific/Invitrogen) and the virus genomes were released from BACs with PacI restriction enzyme (Thermo Scientific). The genomes were transfected into A549 cells with Lipofectamine 2000 reagent (Invitrogen) according to the manufacturer's instructions.

The viruses were purified with cesium chloride gradient centrifugation. VP concentration was determined with optical density 260 (OD_{260}) reading and infectious units by the tissue culture infectious dose (TCID50) assay. The functionality of the viruses was confirmed by infecting human and hamster cancer cell lines and measuring cell viability with the MTS assay by adding 10% CellTiter 96 AQueous One Solution (Promega) for the cells and reading the absorbance at 490 nm after 2 hr. Functionality assays were repeated at least once.

Cytokine Expression and Biological Activity

A549, SKOV3-Luc, HapT1, and DDT1-MF2 cells were infected for 72 hr. Human IL-2 and TNF-α were detected from cell supernatants using the BD Cytometric Bead Array Human Soluble Protein Master Buffer Kit together with human IL-2 and TNF-α Flex Sets (BD) according to the manufacturer's instructions. The beads were detected with a BD Accuri Flow Cytometer and the results were analyzed with FCAP Array software (version 3.0.1; BD Biosciences).

Biological activity of the cytokines was confirmed with IL-2-dependent CTLL-2 cells or TNF-α-sensitive L929 cells. CTLL-2 cells were cultured with filtered supernatants or recombinant human IL-2

(R&D Systems) 10 ng/mL at +37°C and 5% CO_2 for 72 hr. For TNF-α activity experiments, L929 cells were incubated with cell growth media supernatants or 0.5 ng/mL recombinant human TNF-α (R&D Systems) together with 2 μg/mL actinomycin D for 24 hr. In both assays, viable cells were detected with the MTS assay.

In vivo cytokine expression was examined by injecting established HapT1 tumors with 1×10^8 VPs 48 hr before collection. Human IL-2 and TNF-α levels in serum and in homogenized tumors were quantified with a cytometric bead array and normalized to total protein content.

TIL Extraction and Ex Vivo Killing Assay

Subcutaneous HapT1 tumors established on Syrian hamsters (*Mesocricetus auratus*, HsdHan:AURA; Envigo) were allowed to develop for 10 days. Tumor fragments (1–3 mm^3) were cultured in G-Rex10 (Wilson Wolf) in the presence of 3,000 IU/mL human IL-2 (PeproTech). Half of the medium was replaced with fresh medium containing 1 μg/mL concanavalin A (Con A) (Sigma-Aldrich) after 5 days and every other day thereafter until day 10. Fresh TILs were employed in animal experiments or in an ex vivo killing assay, where HapT1 cells were infected with 5,000 VPs per cell for 72 hr before adding 2.5×10^4 TILs extracted from HapT1 tumors. Cell viability was measured with the MTS assay 24 hr after adding TILs.

Animal Experiments

The Experimental Animal Committee of the University of Helsinki and the Provincial Government of Southern Finland approved the animal experiments performed in this study. The animals were under isoflurane anesthesia during all procedures. Immunocompromised female CB-17 SCID mice (Janvier Labs), aged 4–6 weeks, received 5×10^6 SKOV3-Luc cells intraperitoneally. To investigate the effect of different dosing of the virus, the animals were divided to four groups (n = 3) and treated with Ad5/3-E2F-d24-hTNFa-IRES-hIL2 in concentrations of 1×10^5, 1×10^7, or 1×10^9 VPs in 300 μL PBS intraperitoneally. The control group received PBS.

Animals were imaged once a week with an IVIS 100 imaging system (Xenogen). Three milligrams of D-luciferin (Synchem) in 100 μL PBS was administered intraperitoneally 8 minutes before bioluminescent imaging as previously described.[48] To explore the differences in efficacy of the viruses in vivo, the mice were randomized into groups of five to seven mice and treated with 1×10^9 VPs in 300 μL PBS intraperitoneally or PBS alone once a week.

Subcutaneous HapT1 tumors (2×10^6 cells per tumor) were established in 5- to 6-week-old immunocompetent male Syrian hamsters. When the average tumor diameter reached 0.5 cm, the animals were randomized into groups of six to seven. Intratumoral injection of 1×10^9 VPs in 50 μL PBS or PBS alone was performed. Viral treatments were repeated on days 4, 8, 13, and 19. On day 2, hamsters received intratumoral administration of either 4×10^5 HapT1-derived TILs in 50 μL plain RPMI or media only. Twenty-five days after the treatments began, the animals were euthanized and tumors and selected organs were collected to evaluate the histopathological characteristics and immune cell subsets present. The experiment was repeated with reduced virus dosing (1×10^8 VPs on days 1 and 8).

Cured animals were re-challenged with the same tumors (HapT1) or immunologically distinct tumors (DDT1-MF2) (4×10^6 cells/tumor) after a 2-week rest period. Tumor growth was followed for 18 days until DDT1-MF2 tumors reached the maximum tolerated diameter (2 cm).

Flow Cytometric Analyses and Splenocyte Proliferation

$CD8b^+$, $CD4^+$, and MHC class II^+ cells were detected from hamster tumors, spleens, and lymph nodes as described by Siurala et al.[39] Polyclonal anti-Asialo-GM1 AF488 antibody (eBioscience) was used for detecting natural killer cells and a subset of monocytes/macrophages (0.5 μg per reaction) and anti-human/mouse Galectin-3 (Mac-2) PE (eBioscience) for detecting macrophages and dendritic cells (0.2 μg per reaction). In addition, hamster splenocytes from each treatment group were pooled and assessed for proliferation after 72 hr of cultivation. Cell count was determined with a BD Accuri Flow Cytometer.

Histopathology

Tumor samples along with tissue samples from the hamster heart, lung, liver, spleen, and kidney were collected for pathological evaluation. Samples were fixed in 10% formalin for 48 hr and stored in 70% ethanol until histological processing. Sections at 4-μm thickness were cut from paraffin blocks and the slides were stained with hematoxylin and eosin. A veterinary pathologist evaluated histological changes from the stained samples. Tumors lacking neoplastic cells were considered cured.

Statistical Analyses

Differences between groups were estimated with the two-tailed Student's t test, non-parametric Mann-Whitney test, or ANOVA with GraphPad Prism software (version 6.05). IBM SSPS Statistics software (version 22.0.0.1) was utilized when analyzing log-transformed tumor volume data from hamster experiment using a linear mixed-effects model and for analyzing the curative effect of TILs with the Wilcoxon signed-rank test. Differences were considered statistically significant when $p < 0.05$.

SUPPLEMENTAL INFORMATION

Supplemental Information includes Supplemental Materials and Methods, three figures, and one appendix and can be found with this article online at http://dx.doi.org/10.1016/j.omto.2016.12.004.

AUTHOR CONTRIBUTIONS

R.H., M.S., S.P., S.T., and A.H. designed the study. R.H., M.S., S.P., S.T. and M.B. developed the methodology. D.M.N., A.E., and A.K. provided materials for the experiments that were performed by R.H., M.S., S.G.-V.-K., S.T., J.M.S., and J.R. R.H. and P.K. analyzed the data. All authors have reviewed the manuscript.

CONFLICTS OF INTEREST

R.H. has been supported by the University of Helsinki Doctoral Programme in Clinical Research. A.H. received grants from Helsinki University Central Hospital (HUCH) Research Funds, the Sigrid Juselius Foundation, Biocentrum Helsinki, Biocenter Finland, and Finnish Cancer Organizations, and he is a Jane and Aatos Erkko Professor of Oncology at the University of Helsinki. In addition, A.H. is a shareholder in Targovax ASA and an employee and a shareholder in TILT Biotherapeutics, Ltd. M.S., S.P., and J.M.S. are employees of TILT Biotherapeutics, Ltd. The other authors declare no potential conflicts of interest.

ACKNOWLEDGMENTS

We thank the Biomedicum Imaging Unit (BIU) and FACS Core Facility of Biomedicum Helsinki for providing the facilities, technical assistance, and software for in vivo imaging and flow cytometry, respectively. The Finnish Centre for Laboratory Animal Pathology (FCLAP) at the University of Helsinki is acknowledged for histopathological sample processing and evaluation. We thank Majlen Fazer and Paul Ehrnrooth for their donation, as well as the Jane and Aatos Erkko Foundation.

REFERENCES

1. Rosenberg, S.A., Yang, J.C., Sherry, R.M., Kammula, U.S., Hughes, M.S., Phan, G.Q., Citrin, D.E., Restifo, N.P., Robbins, P.F., Wunderlich, J.R., et al. (2011). Durable complete responses in heavily pretreated patients with metastatic melanoma using T-cell transfer immunotherapy. Clin. Cancer Res. *17*, 4550–4557.

2. Larkin, J., Chiarion-Sileni, V., Gonzalez, R., Grob, J.J., Cowey, C.L., Lao, C.D., Schadendorf, D., Dummer, R., Smylie, M., Rutkowski, P., et al. (2015). Combined nivolumab and ipilimumab or monotherapy in untreated melanoma. N. Engl. J. Med. *373*, 23–34.

3. Andtbacka, R.H., Kaufman, H.L., Collichio, F., Amatruda, T., Senzer, N., Chesney, J., Delman, K.A., Spitler, L.E., Puzanov, I., Agarwala, S.S., et al. (2015). Talimogene laherparepvec improves durable response rate in patients with advanced melanoma. J. Clin. Oncol. *33*, 2780–2788.

4. Li, H., Wang, C., Yu, J., Cao, S., Wei, F., Zhang, W., Han, Y., and Ren, X.B. (2009). Dendritic cell-activated cytokine-induced killer cells enhance the anti-tumor effect of chemotherapy on non-small cell lung cancer in patients after surgery. Cytotherapy *11*, 1076–1083.

5. Zhao, X., Zhang, Z., Li, H., Huang, J., Yang, S., Xie, T., Huang, L., Yue, D., Xu, L., Wang, L., et al. (2015). Cytokine induced killer cell-based immunotherapies in patients with different stages of renal cell carcinoma. Cancer Lett. *362*, 192–198.

6. Itzhaki, O., Levy, D., Zikich, D., Treves, A.J., Markel, G., Schachter, J., and Besser, M.J. (2013). Adoptive T-cell transfer in melanoma. Immunotherapy *5*, 79–90.

7. Radvanyi, L.G., Bernatchez, C., Zhang, M., Fox, P.S., Miller, P., Chacon, J., Wu, R., Lizee, G., Mahoney, S., Alvarado, G., et al. (2012). Specific lymphocyte subsets predict response to adoptive cell therapy using expanded autologous tumor-infiltrating lymphocytes in metastatic melanoma patients. Clin. Cancer Res. *18*, 6758–6770.

8. Schwartz, R.N., Stover, L., and Dutcher, J. (2002). Managing toxicities of high-dose interleukin-2. Oncology (Williston Park) *16* (*Suppl 13*), 11–20.

9. Dummer, R., Rochlitz, C., Velu, T., Acres, B., Limacher, J.M., Bleuzen, P., Lacoste, G., Slos, P., Romero, P., and Urosevic, M. (2008). Intralesional adenovirus-mediated interleukin-2 gene transfer for advanced solid cancers and melanoma. Mol. Ther. *16*, 985–994.

10. Parviainen, S., Ahonen, M., Diaconu, I., Kipar, A., Siurala, M., Vähä-Koskela, M., Kanerva, A., Cerullo, V., and Hemminki, A. (2015). GMCSF-armed vaccinia virus induces an antitumor immune response. Int. J. Cancer *136*, 1065–1072.

11. Turnbull, S., West, E.J., Scott, K.J., Appleton, E., Melcher, A., and Ralph, C. (2015). Evidence for oncolytic virotherapy: where have we got to and where are we going? Viruses *7*, 6291–6312.

12. Endo, Y., Sakai, R., Ouchi, M., Onimatsu, H., Hioki, M., Kagawa, S., Uno, F., Watanabe, Y., Urata, Y., Tanaka, N., and Fujiwara, T. (2008). Virus-mediated oncolysis induces danger signal and stimulates cytotoxic T-lymphocyte activity via proteasome activator upregulation. Oncogene *27*, 2375–2381.

13. Bramante, S., Kaufmann, J.K., Veckman, V., Liikanen, I., Nettelbeck, D.M., Hemminki, O., Vassilev, L., Cerullo, V., Oksanen, M., Heiskanen, R., et al. (2015). Treatment of melanoma with a serotype 5/3 chimeric oncolytic adenovirus coding for GM-CSF: results in vitro, in rodents and in humans. Int. J. Cancer *137*, 1775–1783.

14. Khammari, A., Nguyen, J.M., Saint-Jean, M., Knol, A.C., Pandolfino, M.C., Quereux, G., Brocard, A., Peuvrel, L., Saiagh, S., Bataille, V., et al. (2015). Adoptive T cell therapy combined with intralesional administrations of TG1042 (adenovirus expressing interferon-γ) in metastatic melanoma patients. Cancer Immunol. Immunother. *64*, 805–815.

15. Tähtinen, S., Blattner, C., Vähä-Koskela, M., Saha, D., Siurala, M., Parviainen, S., Utikal, J., Kanerva, A., Umansky, V., and Hemminki, A. (2016). T cell therapy enabling adenoviruses coding for IL2 and TNF-α induce systemic immunomodulation in mice with spontaneous melanoma. J. Immunother. *39*, 343–354.

16. Tähtinen, S., Kaikkonen, S., Merisalo-Soikkeli, M., Grönberg-Vähä-Koskela, S., Kanerva, A., Parviainen, S., Vähä-Koskela, M., and Hemminki, A. (2015). Favorable alteration of tumor microenvironment by immunomodulatory cytokines for efficient T-cell therapy in solid tumors. PLoS ONE *10*, e0131242.

17. Siurala, M., Havunen, R., Saha, D., Lumen, D., Airaksinen, A.J., Tahtinen, S., Cervera-Carrascon, V., Bramante, S., Parviainen, S., Vähä-Koskela, M., et al. (2016). Adenoviral delivery of tumor necrosis factor-alpha and interleukin-2 enables successful adoptive cell therapy of immunosuppressive melanoma. Mol. Ther. *24*, 1435–1443.

18. Rosenberg, S.A. (2014). IL-2: the first effective immunotherapy for human cancer. J. Immunol. *192*, 5451–5458.

19. Weide, B., Derhovanessian, E., Pflugfelder, A., Eigentler, T.K., Radny, P., Zelba, H., Pföhler, C., Pawelec, G., and Garbe, C. (2010). High response rate after intratumoral treatment with interleukin-2: results from a phase 2 study in 51 patients with metastasized melanoma. Cancer *116*, 4139–4146.

20. Trudel, S., Trachtenberg, J., Toi, A., Sweet, J., Li, Z.H., Jewett, M., Tshilias, J., Zhuang, L.H., Hitt, M., Wan, Y., et al. (2003). A phase I trial of adenovector-mediated delivery of interleukin-2 (AdIL-2) in high-risk localized prostate cancer. Cancer Gene Ther. *10*, 755–763.

21. Hirvinen, M., Rajecki, M., Kapanen, M., Parviainen, S., Rouvinen-Lagerström, N., Diaconu, I., Nokisalmi, P., Tenhunen, M., Hemminki, A., and Cerullo, V. (2015). Immunological effects of a tumor necrosis factor alpha-armed oncolytic adenovirus. Hum. Gene Ther. *26*, 134–144.

22. Balkwill, F. (2009). Tumour necrosis factor and cancer. Nat. Rev. Cancer *9*, 361–371.

23. Mocellin, S., Rossi, C.R., Pilati, P., and Nitti, D. (2005). Tumor necrosis factor, cancer and anticancer therapy. Cytokine Growth Factor Rev. *16*, 35–53.

24. Heise, C., Hermiston, T., Johnson, L., Brooks, G., Sampson-Johannes, A., Williams, A., Hawkins, L., and Kirn, D. (2000). An adenovirus E1A mutant that demonstrates potent and selective systemic anti-tumoral efficacy. Nat. Med. *6*, 1134–1139.

25. Fueyo, J., Gomez-Manzano, C., Alemany, R., Lee, P.S., McDonnell, T.J., Mitlianga, P., Shi, Y.X., Levin, V.A., Yung, W.K., and Kyritsis, A.P. (2000). A mutant oncolytic adenovirus targeting the Rb pathway produces anti-glioma effect in vivo. Oncogene *19*, 2–12.

26. Kanerva, A., Zinn, K.R., Chaudhuri, T.R., Lam, J.T., Suzuki, K., Uil, T.G., Hakkarainen, T., Bauerschmitz, G.J., Wang, M., Liu, B., et al. (2003). Enhanced therapeutic efficacy for ovarian cancer with a serotype 3 receptor-targeted oncolytic adenovirus. Mol. Ther. *8*, 449–458.

27. Hemminki, O., Parviainen, S., Juhila, J., Turkki, R., Linder, N., Lundin, J., Kankainen, M., Ristimäki, A., Koski, A., Liikanen, I., et al. (2015). Immunological data from cancer patients treated with Ad5/3-E2F-Δ24-GMCSF suggests utility for tumor immunotherapy. Oncotarget *6*, 4467–4481.

28. Koski, A., Bramante, S., Kipar, A., Oksanen, M., Juhila, J., Vassilev, L., Joensuu, T., Kanerva, A., and Hemminki, A. (2015). Biodistribution analysis of oncolytic

adenoviruses in patient autopsy samples reveals vascular transduction of noninjected tumors and tissues. Mol. Ther. *23*, 1641–1652.

29. Disis, M.L. (2014). Mechanism of action of immunotherapy. Semin. Oncol. *41* (*Suppl 5*), S3–S13.

30. Tähtinen, S., Grönberg-Vähä-Koskela, S., Lumen, D., Merisalo-Soikkeli, M., Siurala, M., Airaksinen, A.J., Vähä-Koskela, M., and Hemminki, A. (2015). Adenovirus improves the efficacy of adoptive T-cell therapy by recruiting immune cells to and promoting their activity at the tumor. Cancer Immunol. Res. *3*, 915–925.

31. Balza, E., Carnemolla, B., Mortara, L., Castellani, P., Soncini, D., Accolla, R.S., and Borsi, L. (2010). Therapy-induced antitumor vaccination in neuroblastomas by the combined targeting of IL-2 and TNFalpha. Int. J. Cancer *127*, 101–110.

32. Kuei, J.H., Tashkin, D.P., and Figlin, R.A. (1989). Pulmonary toxicity of recombinant human tumor necrosis factor. Chest *96*, 334–338.

33. Russell, S.J., Peng, K.W., and Bell, J.C. (2012). Oncolytic virotherapy. Nat. Biotechnol. *30*, 658–670.

34. Liikanen, I., Monsurrò, V., Ahtiainen, L., Raki, M., Hakkarainen, T., Diaconu, I., Escutenaire, S., Hemminki, O., Dias, J.D., Cerullo, V., et al. (2011). Induction of interferon pathways mediates in vivo resistance to oncolytic adenovirus. Mol. Ther. *19*, 1858–1866.

35. Yan, Y., Li, S., Jia, T., Du, X., Xu, Y., Zhao, Y., Li, L., Liang, K., Liang, W., Sun, H., and Li, R. (2015). Combined therapy with CTL cells and oncolytic adenovirus expressing IL-15-induced enhanced antitumor activity. Tumour Biol. *36*, 4535–4543.

36. Nishio, N., Diaconu, I., Liu, H., Cerullo, V., Caruana, I., Hoyos, V., Bouchier-Hayes, L., Savoldo, B., and Dotti, G. (2014). Armed oncolytic virus enhances immune functions of chimeric antigen receptor-modified T cells in solid tumors. Cancer Res. *74*, 5195–5205.

37. Thomas, M.A., Spencer, J.F., La Regina, M.C., Dhar, D., Tollefson, A.E., Toth, K., and Wold, W.S. (2006). Syrian hamster as a permissive immunocompetent animal model for the study of oncolytic adenovirus vectors. Cancer Res. *66*, 1270–1276.

38. Gowen, B.B., Judge, J.W., Wong, M.H., Jung, K.H., Aylsworth, C.F., Melby, P.C., Rosenberg, B., and Morrey, J.D. (2008). Immunoprophylaxis of Punta Toro virus (Phlebovirus, Bunyaviridae) infection in hamsters with recombinant Eimeria profilin-like antigen. Int. Immunopharmacol. *8*, 1089–1094.

39. Siurala, M., Vähä-Koskela, M., Havunen, R., Tähtinen, S., Bramante, S., Parviainen, S., Mathis, J.M., Kanerva, A., and Hemminki, A. (2016). Syngeneic Syrian hamster tumors feature tumor-infiltrating lymphocytes allowing adoptive cell therapy enhanced by oncolytic adenovirus in a replication permissive setting. OncoImmunology *5*, e1136046.

40. Liao, W., Lin, J.X., and Leonard, W.J. (2013). Interleukin-2 at the crossroads of effector responses, tolerance, and immunotherapy. Immunity *38*, 13–25.

41. Quezada, S.A., Simpson, T.R., Peggs, K.S., Merghoub, T., Vider, J., Fan, X., Blasberg, R., Yagita, H., Muranski, P., Antony, P.A., et al. (2010). Tumor-reactive CD4(+) T cells develop cytotoxic activity and eradicate large established melanoma after transfer into lymphopenic hosts. J. Exp. Med. *207*, 637–650.

42. De Cesaris, P., Starace, D., Riccioli, A., Padula, F., Filippini, A., and Ziparo, E. (1998). Tumor necrosis factor-alpha induces interleukin-6 production and integrin ligand expression by distinct transduction pathways. J. Biol. Chem. *273*, 7566–7571.

43. Tysome, J.R., Li, X., Wang, S., Wang, P., Gao, D., Du, P., Chen, D., Gangeswaran, R., Chard, L.S., Yuan, M., et al. (2012). A novel therapeutic regimen to eradicate established solid tumors with an effective induction of tumor-specific immunity. Clin. Cancer Res. *18*, 6679–6689.

44. Cerullo, V., Pesonen, S., Diaconu, I., Escutenaire, S., Arstila, P.T., Ugolini, M., Nokisalmi, P., Raki, M., Laasonen, L., Särkioja, M., et al. (2010). Oncolytic adenovirus coding for granulocyte macrophage colony-stimulating factor induces antitumoral immunity in cancer patients. Cancer Res. *70*, 4297–4309.

45. Warming, S., Costantino, N., Court, D.L., Jenkins, N.A., and Copeland, N.G. (2005). Simple and highly efficient BAC recombineering using galK selection. Nucleic Acids Res. *33*, e36.

46. Ruzsics, Z., Wagner, M., Osterlehner, A., Cook, J., Koszinowski, U., and Burgert, H.G. (2006). Transposon-assisted cloning and traceless mutagenesis of adenoviruses: development of a novel vector based on species D. J. Virol. *80*, 8100–8113.

47. Mück-Häusl, M., Solanki, M., Zhang, W., Ruzsics, Z., and Ehrhardt, A. (2015). Ad 2.0: a novel recombineering platform for high-throughput generation of tailored adenoviruses. Nucleic Acids Res. *43*, e50.

48. Hemminki, O., Bauerschmitz, G., Hemmi, S., Lavilla-Alonso, S., Diaconu, I., Guse, K., Koski, A., Desmond, R.A., Lappalainen, M., Kanerva, A., et al. (2011). Oncolytic adenovirus based on serotype 3. Cancer Gene Ther. *18*, 288–296.

OMTO, Volume *4*

Supplemental Information

Oncolytic Adenoviruses Armed with Tumor Necrosis Factor Alpha and Interleukin-2 Enable Successful Adoptive Cell Therapy

Riikka Havunen, Mikko Siurala, Suvi Sorsa, Susanna Grönberg-Vähä-Koskela, Michael Behr, Siri Tähtinen, João Manuel Santos, Pauliina Karell, Juuso Rusanen, Dirk M. Nettelbeck, Anja Ehrhardt, Anna Kanerva, and Akseli Hemminki

Finnish Centre for Laboratory Animal Pathology (FCLAP)

ORGAN SAMPLE REPORT

Species: Mesocricetus auratus	**Breed/Strain:**	**FCLAP Lab No(s):** F11951
Age: –	**Sex:** Male	**Bodyweight:** –
Owner/referring scientist: Riikka Havunen		**Study Animal No:** See below
Submitted for: Histological examination and immunohistochemistry		
Study Type and No: Toxicity of different viral treatments		
Date treatment started: variable	**Date of death: 16.11.2015**	**Type of death:** 0 - Scheduled Sacrifice
Billing address:		**Pathologist(s):** Jere Lindén (JKL) **Typed:** JKL
Date received:	**Date of Necropsy:**	**Date of report: 29.4. 2016 (draft)**
Clinical Features: See below		

MATERIALS and METHODS

The samples consisted of selected organs, subcutaneous pancreatic tumour implants and lymph nodes of 51 hamsters, which had been treated with various unspecified anticancer viral treatments.

Animal number	Treatment	Animal number	Treatment
A1 – A6	Control	F1, F3, F4, F5, F6	TIL
B1 – B6	Ad5/3-E2F-d24	G2 – G6	Ad5/3-E2F-d24 + TIL
C1 – C6	Ad5/3-E2F-d24-hTNFa	H2, H3, H5 – H7	Ad5/3-E2F-d24-hTNFa + TIL
D1, D2, D4, D6	Ad5/3-E2F-d24-hIL2	I1, I4, I5, I6	Ad5/3-E2F-d24-hIL2 + TIL
E2, E3, E7	Ad5/3-E2F-d24-hTNFa-IRES-hIL2	J1 – J7	Ad5/3-E2F-d24-hTNFa-IRES-hIL2 + TIL

Specifically, organ samples had been taken from **heart** (whole heart), **lung** (one lobe), **liver** (piece of one lobe), **kidney** (side not reported) and **spleen**. For histopathology samples were trimmed, processed routinely into paraffin blocks, cut at 4 µm, and stained with hematoxylin and eosin. Immunohistological analyses of the pancreatic tumour implant and lymph node samples were conducted using antibodies against CD3 (T-cells) and cleaved caspase 3 (apoptosis)

Microscopic findings were classified with standard pathological nomenclature and their severities were graded on a scale of 1 to 4 as minimal, mild, moderate or marked. Grades of severity for microscopic findings were subjective; mininal was the least extent discernible. Microscopic findings that are not usually graded were recorded as present. In case there were no considerable histological findings a phrase “No histological abnormality is recognized (NHAIR)” was used. Semi-quantitative scoring was also applied to T cells (CD3 positive cells) and apoptosis and/or necrosis (caspase-3). Scorings are in brackets and in red.

Density of T cell infiltration in the tumor samples was scored applying grades from 1 (single/isolated) to 4 (dense infiltration among neoplastic cells and/or in inflammatory-type foci) while scoring from 1 to 3 was utilized in the lymph nodes. In lymph nodes grade 1 was used for a sparse population (still dozens to hundreds of cells) of T cells often residing mainly in one compartment and grade 3 for a large

population often representing half (over half) of lymphocytes in the section. Variability was generally modest in the samples.

Caspase-3 positivity appeared to emerge from necrotic areas, single apoptotic or necrotic cells or (globular) cell remnants often in macrophages; in grading I assessed only recognizable single cells (round, nucleus or nuclear remnants present), omitting overt coagulative necroses, necrotic areas and cell debris. Apoptosis was scored from 1 to 3 based on the average number of apoptotic cells (AP) per five 40x objective fields (high power field; HPF): 1, less than 5/HPF; 2, approximately 5/HP; 3, approximately 10/HPF. The average number/HPF is also reported.

HISTOPATHOLOGY

A detailed description of the microscopic findings in all animals is provided in Appendix 1. In summary, the following changes were observed in the examined organs:

Heart

Hamsters B2, E2, G3 and H7 exhibited focal acute minimal to mild myodegeneration in septal or ventricular wall. These sporadic alterations were most likely induced by local ischemia.

Lung

Lung samples of all hamsters displayed varying atelectasis and acute diffuse hyperaemia, often accompanied by scattered alveolar haemorrhages. Animals A1, A2, B1, F3, F4 and I4 showed an increase of heterophils (neutrophils) in the lung capillaries.

Liver

Typical liver findings were sampling-related acute haemorrhages and tears, and in most animals hepatocytes contained substantial amounts of glycogen.

Animals A5, A6 B2 C2 and I4 exhibited minimal lymphocytic or mixed portal inflammatory cell infiltration, and C3, C6, I6 and J7 a single portal infiltrate. Minimal focal inflammation (sporadic random inflammatory foci consisting of lymphocytes, heterophils, histiocytes and hepatocellular debris) was present in hamster B4. Hamsters F1 and J2 displayed mild, and J3 moderate glycogen depletion.

Spleen

The spleen samples were generally very small, which impeded their assessment. The most important findings were lymphocyte hyperplasia and increased amount of heterophil aggregates in the red pulp. Lymphocyte hyperplasia, consisting of expansion and rounding of lymphatic areas (white pulp) with increase of medium-sized to large lymphocytes and sometimes lymphoblasts was present in minority of cases. In contrast, loose aggregates of heterophils in red pulp, often near marginal zone, occurred in most animals; only pronounced occurrences are reported. One animal, B5, exhibited mild increase of extramedullary erythroid hematopoiesis in the spleen.

Lymphocyte hyperplasia: minimal B1, B2, B4, B6, C2, C3, E2, J6; mild C6

Increased amount of heterophils in the red pulp: mild A1, B4, C1, E2, F3, G2, H7, I4, I6, J3, J6

Kidney

Hamsters B5, F3, G3 and I6 exhibited focal (one to several foci) tubular dilatation associated with little epithelial degeneration and necrosis. The dilated tubules contained small amount of proteinaceous content and sometimes casts and single calcifications. In some cases, single neighboring glomeruli demonstrated slight sclerosis. Hamster G5 displayed a large triangular, sharply demarcated cortical lesion that consisted of two types of alterations: Most tubules had small lumen and basophilic low regenerative epithelium, while some exhibited dilatation and epithelial degeneration with few necrotic cells, and contained copious proteinaceous casts and cell debris. Glomeruli were little affected.
These histopathological findings point to incipient hamster glomerulonephropathy with minimal changes in B5, F3 and I6, mild in G3 and mild-moderate in G5.

FCLAP Lab No F11951

COMMENTS

Histological examination was performed on a range of tissues from 51 hamsters, which had been treated with various unspecified anticancer viral treatments.

Organs

The examined organ samples exhibited various histopathological findings, however, they are most likely (possibly excluding spleen) unrelated to the treatments: In the heart minor, peracute myodegeneration is probably of ischemic origin and might be related to sampling. In the lungs atelectasis is deemed to be a post mortal change, whereas acute hyperaemia and alveolar haemorrhages are considered to be terminal events relating to euthanasia. Mild heterophilic leucostasis in the lung vasculature is also most likely an incidental finding (a common finding in mice). Respectively, in the liver focal minimal to mild inflammation as well as minimal portal inflammatory cell infiltration show no treatment pattern in their emergence and appear thus to be accidental findings [1]. Variation in glycogen content, relative glycogen depletion, is likewise apparently induced by sampling time [1].

Kidney findings in five animals point to incipient (minimal to mild-moderate) hamster glomerulonephropathy [2]. This disease of unknown aetiology and pathogenesis is regarded to be similar to chronic progressive nephropathy (CPN) in rats [2], however, occurring in hamsters more frequently in females than in males; the lesions have thus been graded according to a rat system [3]. In rats some chemicals are known to exacerbate CPN [3], but this appears to be very unlikely in this study.

In the spleen minimal (one mild) lymphocyte hyperplasia appeared to cluster in treatment groups B and C while increased amount of heterophil aggregates in the red pulp seemed to be evenly dispersed among samples. Clustering of the lymphocyte hyperplasia suggests a treatment-related effect, however, the alterations were marginal (and thus possible incidental), and clearly represented a mild reactive response [4,5]. On the other hand, large number of heterophils in the red pulp, especially pronounced in some animals, occurs to be a consistent finding in hamster spleen.

Tumours and lymph nodes

The tumour samples separated into two distinct categories: 1) Those with epithelioid-like cells (ELCs) resembling inflammatory reaction, generally without discernible neoplastic tissue (inflammatory-type) and 2) aggressive carcinomas with large necrotic areas, sometimes with few ELCs and histiocytic inflammation. The origin of the ELCs remains open; some samples show granulomatous inflammation, which might include true epithelioid cells, while degenerative neoplastic cells cannot be excluded.

Based on HE staining the inflammatory cell infiltration within neoplastic tissue consisted generally of heterophils and lymphocytes with variably intense peripheral infiltrates of similar composition. CD-3 positive T cells appeared to be amply present in all samples, with possibly slightly larger presence in inflammatory-type lesions. In contrast, Caspase-3 positive single apoptotic cells (see Materials and methods) seemed to be more prevalent among carcinomatous tissue, excluding treatment group A, than in inflammatory-type lesions. Notably, these estimates are based on cursory examination of individual animal data.

The lymph node samples formed a heterogeneous population with variable sizes and section planes representing unequally the various lymph node substructures. This heterogeneity appears to mainly explain the apparent variability in T cell density among samples. However, this notion is again based on individual animal data without tabulation of grades.

Jere Lindén

29.4.2016

REFERENCES

1. *Maronpot RR, Cullen J, Malarkey DE. (2014). Liver. In: Cesta MF, Herbert RA, Brix A, Malarkey DE, Sills RC (Eds.), National Toxicology Program Nonneoplastic Lesion Atlas. Available: http://ntp.niehs.nih.gov/nnl/hepatobiliary/liver/index.htm [accessed 20.4.2016]*
2. *Percy DH, Barthold, SW. Hamster. In: Pathology of Laboratory Rodents and Rabbits (3rd Ed.) Oxford: Blackwell Publishing; 2007. pp. 179–216.*
3. *Khan KNM., Hard GC, Alden CL. Kidney. In: Haschek and Rousseaux's Handbook of Toxicologic Pathology (3rd Ed.). Boston: Elsevier; 2013. pp. 1667–1773.*
4. *Ward JM, Rehg JE, Morse HC. (2012). Differentiation of rodent immune and hematopoietic system reactive lesions from neoplasias. Toxicologic Pathology, 40(3), 425–434.*
5. *Ramaiah L, Bounous DI, Elmore SA. Hematopoietic System. In: Haschek and Rousseaux's Handbook of Toxicologic Pathology. Elsevier; 2013. pp. 1863–1933.*

APPENDIX 1. Individual microscopic data

Animal	TISSUE	MICROSCOPIC FINDINGS
A1	Heart	No histological abnormality is recognised (NHAIR).
	Lung	Moderate compression atelectasis; mild acute diffuse hyperaemia. Mild increase of heterophils (neutrophils) in the capillaries.
	Liver	Large acute haemorrhage (sampling). Hepatocytes contain abundant amounts of glycogen. NHAIR
	Spleen	The spleen section is approx.1 mm in diameter. It contains one clearly discernible arteriolar lymphatic sheet area with lymphatic follicle and moderate marginal zone with some macrophages. The red pulp has several loose aggregates of granulocytes.
	Kidney	NHAIR
	Tumour	Oval mass approx. 1 cm x 5 mm, without natural borders; large (comprises 1/4 of area) central coagulative necrosis (CN), intact tumour tissue in poles of the section. Neoplastic adenocarcinoma cells form disorganized tubular structures in tightly-packed nests with an inconspicuous to (in some areas) moderately fibrotic stroma. The cells are anaplastic with indistinct cell borders and moderate amount of dense basophilic cytoplasm. Nuclei are oval and large, showing anisokaryosis with coarse chromatin and prominent nucleoli as well as high mitotic rate (10/HPF). Central necrosis branches into tumour tissue and some heterophils and lymphocytes reside amongst neoplastic cells. Peripherally, rests a focal thin infiltrate of mononuclear cells CD3: Abundant number of T cells among neoplastic cells and in the peripheral infiltrate. [3] Casp-3: Approximately 5 AP/HPF (av. 4.8/HPF) in adenocarcinoma areas [2].
A2	Heart	NHAIR
	Lung	Marked atelectasis; mild acute diffuse hyperaemia; focal small haemorrhages. Mild increase of heterophils in the capillaries.
	Liver	Large acute haemorrhage (sampling); mild acute diffuse hyperaemia. NHAIR
	Spleen	Section size approx.1 x 2 mm. NHAIR
	Kidney	NHAIR
	LN	Partial section, size approx. 0,5 mm (two small lymphatic areas amongst lipid, connective tissue and vasculature). Cell-rich; one discernible primary? lymphatic follicle; no foreign cells. CD-3: Dense population T cells in one area, probably paracortex, single cells elsewhere [2].
	Tumour	Round mass approx. 7 x 6 mm; mostly without natural borders, partly bordered by fibrovascular tissue(dermis). Large ramifying central CN comprises1/2 of tumor area; adenocarcinoma cells (see A1) in chords/nests among necrosis; some heterophils and lymphocytes reside amongst neoplastic cells. Peripheral fibroblast proliferation with some small infiltrates of mononuclear cells and heterophils. CD3: Abundant number of T cells among neoplastic cells and in the peripheral infiltrate. [3] Casp-3: Less than 5 AP/HPF (av. 3.8/HPF) in adenocarcinoma areas [1].

A3	Heart	NHAIR
	Lung	Mild to moderate atelectasis; mild acute diffuse hyperaemia. NHAIR
	Liver	Some small acute haemorrhages and tears (sampling). NHAIR
	Spleen	The section is small and partly broken (approx.1 x 3 mm). NHAIR
	Kidney	NHAIR
	LN	Round section through lymph node, size approx. 1 mm. Cell-rich; Three? lymphatic follicles; no foreign cells. CD-3:Dense population of T cells in the centre [3].
	Tumour	Round mass approx. 6 x 6 mm; mostly without natural borders, small area bordered by dermis. Small ramifying central CN and necrotic foci comprise approx. 1/5 of tumour area; adenocarcinoma cells (see A1) in chords/nests among necrosis and some heterophils and lymphocytes reside amongst neoplastic cells. Peripheral fibroblast proliferation with some small infiltrates of heterophils and mononuclear cells. CD3: Modest number T cells among neoplastic cells; in the infiltrate T cells appear to be a minority. [2] Casp-3: Approximately 5 AP/HPF (av. 6.4/HPF) in adenocarcinoma areas [2].

A4	Heart	NHAIR
	Lung	Marked atelectasis; mild acute diffuse hyperaemia. NHAIR
	Liver	Some small acute haemorrhages and tears (sampling). NHAIR
	Spleen	Section size approx.1,5 x 4 mm. NHAIR
	Kidney	NHAIR
	LN	Partial oblique section, size approx. 1 mm. Cell-rich; lymphatic follicles poorly discernible; no foreign cells. CD-3: Sparse population of T cells outside of one large round central area [2].

A5	Heart	NHAIR
	Lung	Mild to moderate atelectasis; mild acute diffuse hyperaemia. NHAIR
	Liver	A haemorrhage and a tear (sampling). Some small leucocyte infiltrates in portal areas; mononuclear cells and heterophils. Mixed portal inflammatory cell infiltrates, minimal.
	Spleen	The section is small and partly broken (approx.1 x 3 mm). NHAIR
	Kidney	NHAIR
	LN	Partial oblique section, size approx. 1 mm. Cell-rich; no lymphatic follicles discernible; no foreign cells. CD-3: Dense population of T cells in one part of the section [2].
	Tumour	Elongated mass approx. 7 x 5 mm; mostly bordered by dermis and muscle. Moderately-sized ramifying CN and necrotic foci comprise approx. 1/3 of tumour area; some heterophils and lymphocytes reside amongst adenocarcinoma cells (see A1). There is peripheral fibroblast proliferation and some moderate-sized infiltrates of heterophils and mononuclear cells (some apparent plasma cells) reside in the periphery. CD3: Moderate number T cells among neoplastic cells; in the infiltrate T cells appear to be a minority [2]. Casp-3: Less than 5 AP/HPF (aver. 2.8/HPF) in adenocarcinoma areas [1].

A6	Heart	NHAIR
	Lung	Marked diffuse atelectasis; mild acute diffuse hyperaemia; focal small haemorrhages. NHAIR
	Liver	Some small acute haemorrhages and tears (sampling). Two portal tracts contain a moderate-sized lymphocytic infiltrates. Lymphocytic portal inflammatory cell infiltrates, minimal.
	Spleen	Section size approx. 1 x 2 mm. NHAIR
	Kidney	NHAIR
	LN	Round section through lymph node, size approx. 1.5 mm.; paracortex medulla?; no foreign cells. CD-3: Dense population of T cells; deep cortical unit and paracortex? [3].
	Tumour	Elongated mass approx. 5 x 3 mm; mostly without natural borders. Extensive ramifying CN comprises approx. 4/5 of tumour area and adenocarcinoma cells (see A1) reside in the periphery of the mass in chords/nests. Some heterophils and few lymphocytes are present amongst neoplastic cells, and infiltrates of heterophils and mononuclear cells in the periphery. CD3: Abundant numbers of T cells among neoplastic cells and in the peripheral infiltrate. [3] Casp-3: Little neoplastic tissue present; appr. 5 AP/HPF in (av. 4/HPF, three fields evaluated) adenocarcinoma areas [2].

B1	Heart	NHAIR
	Lung	Moderate to marked diffuse atelectasis; mild acute diffuse hyperaemia. Mild increase of heterophils in the capillaries.
	Liver	NHAIR
	Spleen	Section size1.5 x 3 mm. Lymphatic areas (white pulp) are slightly expanded and rounded with minor increase of medium-sized lymphocytes. Lymphocyte hyperplasia, minimal.
	Kidney	NHAIR
	LN	Elongated section through lymph node, size approx. 2 x 1 mm.; some follicles, two secondary? and paracortex; no foreign cells. CD-3: Dense population of T cells; deep cortical unit and paracortex? [3].
	Tumour	Elongated mass approx. 5 x 3 mm; partly without natural borders, partly bordered by thin fibrous capsule and possibly degenerative muscle. Extensive ramifying CN comprises approx. 3/4 of tumour area, remaining viable adenocarcinoma foci (see A1) residing in the periphery. In part, the CN is bordered by a rim of tightly packed large cells with distinct cell borders, abundant foamy, vacuolar and/or granular cytoplasm, and small bland isomorphic nuclei (epithelioid cells/activated macrophages or degenerative (transformed) neoplastic cells?; epithelioid-like cells, ELCs). Amongst the ELCs are a few multinucleated giant cells with lacy or foamy eosinophilic cytoplasms (MGC) some of which contain bluish-gray lucent material. Single heterophils and lymphocytes are present amongst neoplastic cells, and moderate-sized infiltrates of mainly lymphocytes (some apparent plasma cells) reside in the periphery. CD3: Abundant numbers of T cells among neoplastic cells and in the peripheral infiltrate. [3] Casp-3: Little neoplastic tissue present; less than 5 AP/HPF (av. 2/HPF) in adenocarcinoma and ELC areas [1].

B2	Heart	A focal eosinophilic area of myodegeneration in the septum.
	Lung	Moderate to marked diffuse atelectasis; moderate acute diffuse hyperaemia; focal small haemorrhages. NHAIR
	Liver	One portal tract contains two moderate-sized lymphocytic infiltrates. (generally small lymphocytes). Lymphocytic portal inflammatory cell infiltrates, minimal.
	Spleen	Section size approx. 2 x 3 mm (triangular). Lymphatic areas (white pulp) are slightly expanded and rounded with minor increase of medium-sized to large lymphocytes and some lymphoblasts. Lymphocyte hyperplasia, minimal.
	Kidney	NHAIR
	LN	Elongated section through lymph node, size approx. 2 x 1 mm.; mainly paracortex?, no definite follicles; no foreign cells. CD-3: Dense population of T cells focally, generally sparse population [2].
	Tumour	Triangular mass, approx. 4 x 3 mm; partly bordered by fibrovascular tissue. Large ramifying CN comprises approx. 1/2 of tumour area and adenocarcinoma cells reside in the periphery. Few heterophils and lymphocytes are present amongst neoplastic cells; modest infiltrates of mononuclear cells and heterophils cells in the periphery. CD3: Abundant numbers of T cells among neoplastic cells and in the peripheral infiltrate. [3] Casp-3: Little neoplastic tissue present; less than 5 AP/HPF (av. 3.5/HPF, four fields evaluated) in adenocarcinoma areas [1].

B3	Heart	NHAIR
	Lung	Moderate diffuse atelectasis; moderate acute diffuse hyperaemia; focal small haemorrhages. NHAIR
	Liver	NHAIR
	Spleen	Section size approx. 1 x 2 mm. NHAIR.
	Kidney	NHAIR
	LN	Elongated section through lymph node, size approx. 2 x 1 mm.; mainly paracortex?, one primary follicle?; no foreign cells. CD-3: Dense population of T cells in a DCU? [3].
	Tumour	Oval mass, approx. 8 x 5 mm; partly bordered by fibrovascular, lipid and muscle tissues. Moderately-sized ramifying CN and necrotic foci comprise approx. 1/4 of tumour area; viable neoplastic areas show typical adenocarcinoma cells and contain some heterophils and few lymphocytes. There is strong peripheral fibroblast proliferation and large infiltrates of lymphocytes and plasma cells, partly in the bordering tissues. Some apparent plasma cells) reside in the periphery. CD3: Abundant numbers of T cells among neoplastic cells; in the infiltrates T cells are a minority (10%?), but abundantly present. [3] Casp-3: Appr. 10 AP/HPF (aver. 11.4/HPF) in adenocarcinoma areas [3].

B4	Heart	NHAIR
	Lung	Moderate diffuse atelectasis; moderate acute diffuse hyperaemia; focal small haemorrhages. NHAIR
	Liver	Slight acute diffuse hyperaemia. Sporadic random inflammatory foci consisting of lymphocytes, heterophils, histiocytes and hepatocellular debris. Minimal focal inflammation.
	Spleen	Section size approx.1,5 x 4 mm. Lymphatic areas (white pulp) are slightly expanded and rounded with minor increase of medium-sized to large lymphocytes. Lymphocyte hyperplasia, minimal. The red pulp contains mildly increased amounts of heterophil aggregates.
	Kidney	NHAIR

B5	Heart	NHAIR
	Lung	Moderate to marked diffuse atelectasis; moderate acute diffuse hyperaemia; focal small haemorrhages. NHAIR
	Liver	One small inflammatory foci surrounded by degenerated hepatocytes and consisting of lymphocytes and single macrophages. NHAIR
	Spleen	Section size approx.1.5 x 3 mm. Mildly increased extramedullary erythroid haematopoiesis.
	Kidney	Superficial cortex contains three foci (convoluted tubule segments of single nephrons?) of tubular dilatation associated with minimal epithelial degeneration and necrosis.
	LN	Elongated size approx. 3 x 2 mm., lacerated; mainly lymphatic tissue, two secondary follicles; no foreign cells. CD-3: Dense population of T cells in paracortex/cortex? [3].
	Tumour	Elongated mass, approx. 8 x 5 mm and a round 2 mm satellite nodule; both partly bordered by fibrovascular tissue and muscle. In the mass large ramifying CN comprises approx. 1/2 of tumour area and adenocarcinoma cells reside in the periphery; nodule consists of adenocarcinoma with small necrotic foci. Some heterophils and few lymphocytes are present amongst neoplastic cells; modest infiltrates of mononuclear cells and heterophils (more heterophils in the large mass) in the periphery and moderate peripheral fibroblast proliferation in the mass. CD3: Abundant numbers of T cells among neoplastic cells and in the peripheral infiltrate. [3] Casp-3: Approximately 5 AP/HPF (av. 6/HPF) in adenocarcinoma areas [2].

B6	Heart	NHAIR
	Lung	Moderate diffuse atelectasis with areas of marked diffuse atelectasis; moderate acute diffuse hyperaemia. NHAIR
	Liver	Focal small superficial haemorrhages. NHAIR
	Spleen	Section size approx. 1 x 4 mm. Lymphocyte hyperplasia, minimal. (see B4).
	Kidney	NHAIR
	LN	Round section through lymph node, size approx. 1 mm.; cell dense, mainly paracortex?, three follicles?; no foreign cells. CD-3: Dense population of T cells in a DCU/paracortex? [3].
	Tumour	Elongated mass approx. 4 x 3 mm; partly without natural borders, partly bordered by thin fibrous capsule. Extensive ramifying CN comprises approx. 2/3 of tumour area, remaining viable adenocarcinoma residing in the periphery. Large number of heterophils and some lymphocytes are present amongst neoplastic cells, and large infiltrates of mainly lymphocytes (some apparent plasma cells) and some heterophils reside in the periphery. CD3: Moderate number T cells among neoplastic cells and in the infiltrate. [2] Casp-3: Little neoplastic tissue present. Aproximately 5 AP/HPF (aver. 6.2/HPF) in adenocarcinoma areas [2].

C1	Heart	NHAIR
	Lung	Moderate diffuse atelectasis; moderate acute diffuse hyperaemia. NHAIR
	Liver	Focal small superficial haemorrhages. One inflammatory focus consisting of heterophils, histiocytes, lymphocytes and hepatocellular debris. NHAIR
	Spleen	Section size approx. 1 x 3 mm. Mildly increased number of loose granulocyte aggregates in the red pulp.
	Kidney	NHAIR
	LN	Elongated size approx. 3 x 2 mm; cortex, paracortex and medulla; no foreign cells. CD-3: Dense population of T cells [3].
	Tumour	Round mass, approx. 3 mm; without natural borders. Moderate-sized CN comprises approx. 1/3 of tumour area, remaining viable adenocarcinoma flanks the CN and contains several small necrotic foci. Some heterophils and lymphocytes are present amongst neoplastic cells, but there are very infiltrates of mainly lymphocytes (some apparent plasma cells) and some heterophils reside in the periphery. CD3: Moderate number T cells among neoplastic cells and in the infiltrate. [2] Casp-3: Appr.10 AP/HPF (av. 9.8/HPF) in adenocarcinoma areas [3].

C2	Heart	NHAIR
	Lung	Moderate diffuse atelectasis; moderate acute diffuse hyperaemia. NHAIR
	Liver	Focal small superficial haemorrhages. One large portal lymphocytic infiltrate. Lymphocytic portal inflammatory cell infiltrates, minimal.
	Spleen	Section size approx. 1.5 x 3 mm. One coalescing area of white pulp that is slightly expanded and rounded with increased number of medium-sized to large lymphocytes. Lymphocyte hyperplasia, minimal.
	Kidney	NHAIR
	LN	Round section through lymph node, size approx. 2 mm.; cell dense, mainly paracortex and cortex?, some follicles?; no foreign cells. CD-3: Very sparse population of T cells [1].

C3	Heart	NHAIR
	Lung	Moderate, focally mild, atelectasis; moderate acute diffuse hyperaemia. NHAIR
	Liver	Focal small superficial haemorrhages and tears. One medium-sized portal lymphocytic infiltrate. NHAIR
	Spleen	Section size approx. 1 x 3 mm. Lymphatic areas (white pulp) are mildly expanded and rounded with some increase of medium-sized to large lymphocytes. Lymphocyte hyperplasia, mild.
	Kidney	NHAIR
	LN	Elongated section, size approx. 2 x 1 mm; cortex +paracortex, hilus in the middle?, activated: four secondary follicles; no foreign cells. CD-3: Sparse population of T cells mainly in cortex [1].

C4	Heart	NHAIR
	Lung	Moderate to marked atelectasis; moderate acute diffuse hyperaemia. NHAIR
	Liver	Focal small superficial haemorrhages. NHAIR
	Spleen	Section size approx. 1 x 5 mm. NHAIR
	Kidney	NHAIR
	LN	Round section, size approx. 2 mm; cortex, paracortex and medulla?, activated: 4-5 secondary follicles; no foreign cells. CD-3: T cells in cortex and in paracortex (DCU) [2].

C5	Heart	NHAIR
	Lung	Marked atelectasis; moderate acute diffuse hyperaemia; multifocal small alveolar haemorrhages. NHAIR
	Liver	Focal haemorrhages and tears. NHAIR
	Spleen	Section size approx. 1 x 3 mm. NHAIR
	Kidney	NHAIR
	LN	Elongated section, size approx. 3 x 2 mm; cortex, paracortex and medulla?, activated: 3 secondary follicles; no foreign cells. CD-3: Sparse T cells mainly in cortex [2].

C6	Heart	NHAIR
	Lung	Marked atelectasis; moderate acute diffuse hyperaemia. NHAIR
	Liver	Focal haemorrhages and tears. One medium-sized portal lymphocytic infiltrate. NHAIR
	Spleen	Section size approx. 1 x 6 mm. Lymphatic areas (white pulp) are mildly expanded and with some increase of medium-sized to large lymphocytes. Lymphocyte hyperplasia, mild.
	Kidney	NHAIR
	LN	Round section, size < 1 mm partly crushed; paracortex, one follicle?; no foreign cells. CD-3: Sparse T cells in paracortex? [2].
	Tumour	Size approx. 3 x 2 mm, triangular. Mass consists of epidermis, dermis subcutis and muscle. Subcutaneous-dermal vaguely bordered fibrous tissue without clear adenocarcinoma cells; small aggregates of ELCs and some single MGCs, generally with calcifications. Some loose infiltrates of lymphocytes, plasma cells and few heterophils. CD-3: Moderate amounts of disseminated individual T cells and small aggregates; abundant amount of T cells in ELC aggregates. [3] Casp-3: Less than 5 AP/HPF (aver. 1.6/HPF) in whole section area [1].

D1	Heart	NHAIR
	Lung	Moderate diffuse atelectasis; moderate acute diffuse hyperaemia. NHAIR
	Liver	Focal small superficial haemorrhages. One small portal infiltrate consisting of single lymphocytes and heterophils. NHAIR
	Spleen	Section size approx. 1 x 3 mm. Shrunken white pulp.
	Kidney	NHAIR
	LN	Elongated section, size approx. 2 x 1 mm; cortex, paracortex?, poorly discernible follicles; no foreign cells. CD-3: T cells diffusely [3].

D2	Heart	NHAIR
	Lung	Moderate diffuse atelectasis; moderate acute diffuse hyperaemia. NHAIR
	Liver	Focal small superficial haemorrhages. One small portal infiltrate consisting of lymphocytes and macrophages. NHAIR
	Spleen	Section size approx. 1 x 2 mm. NHAIR
	Kidney	NHAIR

D4	Heart	NHAIR
	Lung	Moderate atelectasis; moderate acute diffuse hyperaemia; focal small haemorrhages. NHAIR
	Liver	A focal haemorrhage and a tear. NHAIR
	Spleen	Section size approx. 1 x 5 mm. NHAIR
	Kidney	NHAIR
	LN	Elongated section, size approx. 3 x 2 mm; cortex +paracortex, hilus in the middle?, poorly discernible follicles; no foreign cells. CD-3: T cells in cortex and in paracortex [2].

D6	Heart	Missing
	Lung	Moderate atelectasis; moderate acute diffuse hyperaemia. NHAIR
	Liver	Focal small superficial haemorrhages. NHAIR
	Spleen	Section size approx. 1 x 4 mm. Lymphocyte hyperplasia, minimal. (See B2)
	Kidney	NHAIR
	LN	Size approx. 1 x 2 mm; superficial cortex and little paracortex; cell-rich, no secondary lymphatic follicles; no foreign cells. CD-3: Some reactivity in paracortex and isolated cells in parafollicular cortex [2].
	Tumour	Size approx. 2 x 2 mm. Partly without natural borders, partly bordered by fibrous tissue containing some degenerative muscle fibres. Reactive tissue? without clear adenocarcinoma cells, main cell type tightly packed ELCs admixed with degenerative heterophils; isolated macropahage-type cells contain yellowish brown granular pigment (hemosiderin); one small peripheral calcified focus with posibble MGCs. CD-3: Large amount of individual T cells and dense T cell aggregates [4]. Casp-3: Less than 5 AP/HPF (av. 1.5/HPF, four areas counted) in ELC areas [1].

E2	Heart	A focal eosinophilic area of acute myodegeneration in the septum.
	Lung	Moderate atelectasis; moderate acute diffuse hyperaemia. NHAIR
	Liver	A focal haemorrhage and tear. NHAIR
	Spleen	Section size approx. 1 x 1.5 mm. The white pulp is slightly expanded and rounded with increased number of medium-sized to large lymphocytes. Lymphocyte hyperplasia, minimal. Mildly increased numbers of heterophils in loose infiltrates in marginal zone.
	Kidney	NHAIR
	LN	Size approx. 1 x 2 mm; cortex and paracortex?; cell-rich, no clear follicles; no foreign cells. CD-3: Little reactivity, mainly in cortex [2].

E2	Tumour	Oval mass, approx. 6 x 4 mm; without natural borders. Large CN comprises approx. 2/3 of tumour area, remaining viable adenocarcinoma flanks the CN and shows abundant fibroplasia. Some heterophils and lymphocytes are present amongst neoplastic cells and in the periphery appears a focal thin infiltrate of heterophils and lymphocytes (some apparent plasma cells). CD3: Moderate number T cells among neoplastic cells and in the infiltrate. [2] Casp-3: Appr. 5 AP/HPF (aver. 7/HPF) in adenocarcinoma areas [3].

E3	Heart	NHAIR
	Lung	Marked atelectasis; moderate acute diffuse hyperaemia. A small subpleural focal infiltrate of heterophils and macrophages surrounded by small haemorrhage. Focal subpleural acute inflammation.
	Liver	A focal haemorrhage and tear. NHAIR
	Spleen	Section size approx. 1 x 3 mm. NHAIR
	Kidney	NHAIR
	LN	Round, approx. 1 mm; cortex and paracortex?; cell-rich, some primary follicles; no foreign cells. CD-3: Dense population of T cells in the paracortex (DCUs?) [3].
	Tumour	A shred of tissue, approx. 1 mm. Fibrous tissue containing some partly calcified necrotic foci, MGCs as well as brown granular pigment (hemosiderin?) and few small lakes of bluish lucent (foreign?) material without cellular reaction; some small infiltrates of lymphocytes and macrophages and individual lymphocytes in the periphery. CD-3: Moderate amounts of disseminated individual T cells and small aggregates [2]. Casp-3: Less than 5 AP/HPF (aver. 1/HPF, three evaluated fields) outside necrotic foci [1].

E7	Heart	NHAIR
	Lung	Marked to moderate atelectasis; moderate acute diffuse hyperaemia; focal small haemorrhages. NHAIR
	Liver	A focal haemorrhage and a tear. NHAIR
	Spleen	Section size approx. 1 x 1 mm. The section contains no white pulp. Mildly increased numbers of heterophils in loose infiltrates in marginal zone.
	Kidney	NHAIR
	LN	Round, approx. 1 mm; cortex and paracortex?; cell-rich, 2 secondary follicles; no foreign cells. CD-3: Modest number of T cells in cortex [2].
	Tumour	Elongated mass, approx. 3 x 2 mm. In fibrous tissue resides an oval (1-2 mm) focus consisting of homogenous eosinophilic material (degenerative collagen), bordered and infiltrated by ELCs as well as some macrophages and lymphocytes. The encircling fibrous tissue contains small infiltrates of lymphocytes and macrophages (few heterophils) and individual lymphocytes; some macrophages contain brown granular pigment (hemosiderin?). CD-3: Moderate amounts of disseminated individual T cells and small aggregates [2]. Casp-3: Less than 5 AP/HPF (aver. 1.2/HPF) in whole section [1].

F1	Heart	NHAIR
	Lung	Moderate to marked atelectasis; moderate acute diffuse hyperaemia; focal alveolar haemorrhages. NHAIR
	Liver	Mild glycogen depletion.
	Spleen	Two sections, both approx. 1 x 2 mm. NHAIR
	Kidney	NHAIR
	LN	Size approx. 1 x 2 mm, perinodal fat and lymphoid tissue; cortex paracortex and medulla?; cell-rich, one secondary follicle; no foreign cells. CD-3: Moderate reactivity, mainly in cortex [2].
	Tumour	Ragged piece of tissue, approx. 3 x 2 mm. Fibrous and fibrovascular tissue and lipid. Some aggregates of foamy ELCs with small lymphocytic infiltrates; peripherally an aggregate of MGCs, lymphocytes and macrophages; small aggregates of lymphocytes and macrophages (some with brow pigment; hemosiderin?); individual lymphocytes / loose infiltrates amply present. CD-3: Ample amount of individual T cells [3]. Casp-3: Less than 5 APHPF (aver. 2.8/HPF, four evaluated fields) in whole section [1].

F3	Heart	NHAIR
	Lung	Marked atelectasis; moderate acute diffuse hyperaemia. Mild increase of heterophils in the capillaries.
	Liver	NHAIR
	Spleen	Section size approx. 1 x 2 mm. Mildly increased numbers of heterophils in loose infiltrates in marginal zone.
	Kidney	Superficial cortex contains one focus (convoluted tubule segment of a single nephron?) of tubule dilatation with proteinaceous content and minimal epithelial degeneration and necrosis accompanied by a degenerative glomerulus with slight sklerosis.
	LN	Elongated section 1 x 2 mm. Cell-rich, paracortex and cortex?; poorly-discernible follicles; no foreign cells. CD-3: Moderate reactivity, mainly in paracortex [3].
	Tumour	Round mass, approx. 8 mm. Mostly without natural borders (a short stretch of fibrous capsule); extensive CN comprises approx. 4/5 of tumour area. Remaining viable adenocarcinoma flanks the CN on one side, showing many small necrotic foci and peripheral moderate fibroplasia. Some lymphocytes are present amongst neoplastic cells; few small infiltrates of heterophils and lymphocytes in outer border of viable tumour and in the fibrous capsule. CD-3: Ample amount of disseminated individual T cells and small aggregates [3]. Casp-3: Approximately 5 AP/HPF (av. 4/HPF) in adenocarcinoma areas [2].

F4	Heart	NHAIR
	Lung	Moderate atelectasis; moderate acute diffuse hyperaemia; mild increase of heterophils in the capillaries.
	Liver	Focal haemorrhages and a tear. NHAIR
	Spleen	Section size approx. 1-2 x 8 mm. Moderately increased numbers of heterophils in loose infiltrates in marginal zones and scattered in the red pulp.
	Kidney	NHAIR
	LN	Partial section of a lymph node, approx. 1 mm. Cell-rich, paracortex and medula?; no discernible follicles; no foreign cells. CD-3: Diffuse reactivity, dense reactivity in a DCU? [3].

F4	Tumour	Triangular section, approx. 6 x 4 mm. Mostly without natural borders, partly bordered by fibrovascular tissue and muscle; CN comprises approx. 1/3 of tumour area. Remaining viable adenocarcinoma flanks the CN on one side, showing many small necrotic foci and moderate fibroplasia. Some lymphocytes are present amongst neoplastic cells and copious infiltrates of heterophils, lymphocytes and plasma cells are present in fibrotic areas and peripherally in tumour borders. CD-3: Ample amount of disseminated individual T cells and T cells in small aggregates [3]. Casp-3: Appr. 5 AP/HPF (aver. 7.4/HPF) in adenocarcinoma areas [2].

F5	Heart	NHAIR
	Lung	Moderate to marked atelectasis; moderate acute diffuse hyperaemia. NHAIR
	Liver	A haemorrhage and a tear. NHAIR
	Spleen	Two sections: approx. 1 x 2 mm. NHAIR
	Kidney	NHAIR

F6	Heart	NHAIR
	Lung	Moderate atelectasis; moderate acute diffuse hyperaemia. NHAIR
	Liver	Focal small superficial haemorrhages. NHAIR
	Spleen	Section size approx. 1 x 6 mm. NHAIR
	Kidney	NHAIR
	Tumour	Round section, approx. 4 mm. Bordered by fibrovascular tissue, muscle or fibrous capsule; Central CN (and a cavity) comprises approx. 2/3 of tumour area. Remaining viable adenocarcinoma surrounds the CN as a thin rim and shows some peripheral fibroplasia. Some lymphocytes are present amongst neoplastic cells and copious infiltrates of heterophils, lymphocytes and plasma cells are circling the tumour borders. CD-3: Ample amount of disseminated individual T cells amongst neoplastic cells and in small aggregates in peripheral infiltrates [3]. Casp-3: Appr.5 AP/HPF (aver. 6.25/HPF, four fields evaluated) in adenocarcinoma areas [1].

G2	Heart	NHAIR
	Lung	Moderate to marked atelectasis; moderate acute diffuse hyperaemia. NHAIR
	Liver	Focal tears and haemorrhages. NHAIR
	Spleen	Section size approx. 1 x 4 mm. Mildly increased numbers of heterophils in loose infiltrates in marginal zone.
	Kidney	NHAIR
	LN	Bean-shaped section of a lymph node, approx. 2 x 1 mm. Cell-rich, all parts present; two secondary follicles?; no foreign cells. CD-3: Dense reactivity in paracortex (a DCU?) [3].

G2	Tumour	Elongated, torn section, approx. 8 x 4 mm. Without natural borders. Extensive CN comprises approx. 4/5 of tumour area. Remaining viable adenocarcinoma flanks the CN on one side, showing many small necrotic foci and some focal fibroplasia. Some lymphocytes are present amongst neoplastic cells, and small infiltrates of heterophils, lymphocytes and plasma cells in the periphery; a focal loose aggregate of ELCs with single calsifications. CD-3: Moderate amount of disseminated individual T cells amongst neoplastic cells and in peripheral infiltrates [2]. Casp-3: Less than 5 AP/ HPF (aver. 2.6/HPF) in adenocarcinoma areas [1].

G3	Heart	Few eosinophilic degenerated myofibers in the left ventricle wall.
	Lung	Moderate to marked atelectasis; moderate acute diffuse hyperaemia. NHAIR
	Liver	One small portal infiltrate consisting of macrophages, lymphocytes and single heterophils. NHAIR
	Spleen	Section size approx. 1 x 2 mm. NHAIR
	Kidney	Cortex contains a few foci of tubular dilatation with epithelial degeneration (and necrosis) or basophilic low regenerative epithelium. Some dilated cortical tubuli and medullary tubular segments contain eosinophilic proteinaceous casts (single calcifications). Few neighbouring glomeruli exhibit slight sclerosis.
	LN	Size approx. 0,3 mm (three small lymphatic areas amongst lipid, connective tissue and vasculature). Cell-rich; no lymphatic follicles no foreign cells. CD-3:Dense positivity in two areas, probably paracortex [3].
	Tumour	Triangular, torn section, approx. 3 mm. Mostly without natural borders, in part bordered by fibrovascular tissue. Large CN and degenerative collagen? comprise approx. 3/4 of tumour area. Remaining viable adenocarcinoma cells form a thin rim on one side and show degenerative changes, small necrotic foci and apoptosis; aggregates of ELCs side the neoplastic cells and there is a peripherial large calcified focus with some MGCs. Large number of heterophils and some lymphocytes are present amongst neoplastic cells; dense infiltrates of heterophils, lymphocytes and plasma cells encircle and invade neoplastic, ELC and calcified areas. CD-3: Abundant amount of disseminated individual T cells amongst neoplastic cells and in peripheral infiltrates [3]. Casp-3: Less than 5 AP/HPF (aver. 1.8/HPF) in adenocarcinoma and ELC areas [1].

G4	Heart	NHAIR
	Lung	Mild to moderate atelectasis; moderate acute diffuse hyperaemia. NHAIR
	Liver	A focal tear and haemorrhage. One medium-sized portal lymphocytic infiltrate with some macrophages. NHAIR
	Spleen	Section size approx. 1 x 6 mm. NHAIR
	Kidney	NHAIR
	LN	Size approx. 0,5 mm, three small lymphatic areas (one crushed) amongst lipid, connective tissue and vasculature. Cell-rich; no lymphatic follicles no foreign cells. CD-3: Sparse population of T cells [2].

G5	Heart	NHAIR
	Lung	Moderate to marked atelectasis; moderate acute diffuse hyperaemia. NHAIR
	Liver	A haemorrhage and a tear. NHAIR
	Spleen	Two sections: approx. 1 x 2 mm. NHAIR
	Kidney	Kidney cortex contains an elongated (2–3 mm) triangular sharply demarcated lesion area with sunken surface. The area consists of densely packed tortuous tubules of two types: Some tubuli are dilated, contain eosinophilic (proteinacous) casts and/or cell debris and show epithelial degeneration with few necrotic cells. The other type of tubules have small lumen and basophilic low regenerative epithelium. Glomeruli are not markedly altered.
	LN	Elongated section, approx. 2 x 1 mm. Cell-rich; little cortex present no discernible lymphatic follicles; no foreign cells. CD-3: Sparse population of T cells [2].

G6	Heart	NHAIR
	Lung	Moderate atelectasis; moderate acute diffuse hyperaemia. NHAIR
	Liver	Focal small superficial haemorrhages. NHAIR
	Spleen	Section size approx. 1 x 6 mm. NHAIR
	Kidney	NHAIR
	LN	Elongated section, approx. 3 x 2 mm. Cell-rich, all parts present; five secondary follicles (activated); no foreign cells. CD-3: Dense reactivity in paracortex (2 DCUs?) [3].
	Tumour	Elongated section, approx. 6 x 4 mm. Bordered by fibrovascular tissue and fibrous capsule. Large ramifying central CN comprises approx. 3/4 of tumour area. Remaining viable adenocarcinoma cells form a thin cap on one side and show small necrotic foci and apoptosis; small aggregates of ELCs side the neoplastic cells and on opposite side exist some MCGs and small calsifications. Some heterophils and lymphocytes are present amongst neoplastic cells; dense infiltrates of heterophils, lymphocytes and plasma cells encircle (in fibrous outer tissue) and invade the neoplastic, ELC and MCG areas. CD-3: Abundant amount of disseminated individual T cells amongst neoplastic cells and in peripheral infiltrates [3]. Casp-3: Approximately 5 AP/HPF (aver. 4.2/HPF) in adenocarcinoma areas [2].

H2	Heart	NHAIR
	Lung	Moderate to marked atelectasis; moderate acute diffuse hyperaemia; focal alveolar haemorrhages. NHAIR
	Liver	NHAIR
	Spleen	Section size approx. 1 x 1.5 mm. NHAIR. Hypoplasia?
	Kidney	NHAIR
	LN	Round approx. 1 mm. Cell-rich; no lymphatic follicles cortex absent?; no foreign cells. CD-3: Even, moderately dense population of T cells [2].

H3	Heart	NHAIR
	Lung	Moderate atelectasis; moderate acute diffuse hyperaemia. NHAIR
	Liver	A haemorrhage and a tear. NHAIR
	Spleen	Section size approx. 1 x 7 mm. NHAIR
	Kidney	NHAIR

H5	Heart	NHAIR
	Lung	Mild atelectasis; moderate acute diffuse hyperaemia. NHAIR
	Liver	A focal tear and haemorrhage. NHAIR
	Spleen	Section size approx. 2 x 3 mm (triangular). NHAIR
	Kidney	NHAIR
	LN	Bean-shaped section of a lymph node, approx. 2 x 1 mm. Cell-rich, all parts present; 2-3 primary follicles?; no foreign cells. CD-3: Sparse population of T cells below cortex [2].

H6	Heart	NHAIR
	Lung	Moderate to marked atelectasis; moderate acute diffuse hyperaemia. NHAIR
	Liver	A haemorrhage and a tear. One small portal lymphocytic infiltrate. NHAIR
	Spleen	Section size approx. 1 x 2 mm (triangular); flaked section. NHAIR
	Kidney	NHAIR

H7	Heart	Two eosinophilic foci of myodegeneration in the septum.
	Lung	Moderate atelectasis; moderate acute diffuse hyperaemia. NHAIR
	Liver	A haemorrhage and a tear. NHAIR
	Spleen	Section size approx. 2 x 3 mm); partly broken. Mildly increased numbers of heterophils in loose aggreagates in the red pulp.
	Kidney	NHAIR
	LN	Bean-shaped section, approx. 2 x 1 mm. Cell-rich, medulla, paracortex, one follicle? no foreign cells. CD-3: Sparse population of T cells below cortex [2].
	Tumour	Round section, approx. 6 mm. Mostly without natural borders; short segment of lipid tissue. Extensive ramifying CN comprises over 4/5 of tumour area. Remaining viable adenocarcinoma cells form a thin cap on one side and small islands on the CN, and show small necrotic foci and apoptosis. Large number of heterophils and some lymphocytes are present amongst neoplastic cells; some small but dense infiltrates of heterophils, lymphocytes and plasma cells flank and invade neoplastic cells. CD-3: Abundant amount of disseminated individual T cells amongst neoplastic cells and in peripheral infiltrates [3]. Casp-3: Little viable tissue; appr. 5 AP/HPF (av. 5.5/HPF, four fields counted) in adenocarcinoma areas [2].

I1	Heart	NHAIR
	Lung	Moderate to marked atelectasis; moderate acute diffuse hyperaemia. NHAIR
	Liver	A haemorrhage and a tear. NHAIR
	Spleen	Section size approx. 1 x 7 mm. Lymphocyte hyperplasia, minimal.

I1	Kidney	NHAIR
	LN	Elongated section, approx. 2 x 1 mm. Cell-rich, cortex, paracortex, 2-3 large secondary follicles; no foreign cells. CD-3: Sparse population of T cells in interfollicular cortex and below cortex [2].
	Tumour	Elongated piece of tissue, approx. 3 x 1 mm. Muscle in one end, other parts without natural borders; fibrous tissue. Some aggregates of foamy ELCs with small lymphocytic infiltrates and areas of MGCs and calcifications; individual lymphocytes / loose lymphocyte infiltrates amply present. CD-3: Moderate amount of T cells individually and in loose aggregates [2]. Casp-3: Little tissue; less than 5 AP/HPF (aver. 0.75/HPF, four fields counted) [1].

I4	Heart	NHAIR
	Lung	Marked atelectasis; moderate acute diffuse hyperaemia; mild increase of heterophils in the capillaries.
	Liver	A haemorrhage and a tear. One large portal (spreading periportally) lymphocytic infiltrate. Lymphocytic portal inflammatory cell infiltrates, minimal.
	Spleen	Section size approx. 1 x 2 mm. Mildly increased numbers of heterophils in the red pulp and in marginal zones.
	Kidney	NHAIR
	LN	Round section, approx. 3 mm. Cell-rich, cortex, paracortex, four secondary follicles; no foreign cells. CD-3: Sparse population of T cells in cortex and below cortex [2].

I5	Heart	NHAIR
	Lung	Marked atelectasis; moderate acute diffuse hyperaemia. NHAIR
	Liver	A haemorrhage and a tear. NHAIR
	Spleen	Section size approx. 1 x 7 mm. Lymphocyte hyperplasia, minimal.
	Kidney	NHAIR
	LN	Elongated, partial section of lymphnode, approx. 3 x 1 mm. Cell-rich, cortex, paracortex, four secondary follicles; no foreign cells. CD-3: Abundant number of T cells in cortex and below cortex (DCU?) [3].

I6	Heart	NHAIR
	Lung	Moderate to marked atelectasis; moderate acute diffuse hyperaemia. NHAIR
	Liver	One medium-sized portal lymphocytic infiltrate with some macrophages. NHAIR
	Spleen	Section size approx. 1 x 2 mm. Mildly increased numbers of heterophils in the red pulp and in marginal zones.
	Kidney	Superficial cortex contains one focus (convoluted tubule segment of a single nephron?) of tubule dilatation with little proteinacous content and minimal epithelial degeneration and necrosis accompanied by a glomerulus with slight mesangial proliferation.
	LN	Elongated, partial section of lymphnode, approx. 3 x 1 mm; some crushing. Cell-rich, mainly paracortex; no foreign cells. CD-3: Very sparse T cell reactivity [1].

J1	Heart	NHAIR
	Lung	Moderate to marked atelectasis; moderate acute diffuse hyperaemia. NHAIR
	Liver	A haemorrhage and a tear. NHAIR
	Spleen	Section size approx. 1 x 7 mm. NHAIR
	Kidney	NHAIR
	LN	Elongated section, approx. 2 x 1 mm, two partial sections of lymphocytes. Cell-rich, paracortex, medulla?, poorly discernible cortex; no foreign cells. CD-3: Dense population of T cells in paracortex (a DCU?and below cortex [3].
	Tumour	Round section, approx. 3 mm. Muscle in one end, other parts without natural borders; fibrous tissue. Large aggregates/infiltrates of foamy ELCs with abundant lymphocyte infiltration; admixed with MGCs and calcifications (and some lucent bluish-gray material); large number of individual lymphocytes and plasma cells / loose lymphocyte infiltrates and macrophages. CD-3: Large number of T cells individually and in loose aggregates especially among ELC aggregates [3]. Casp-3: Heterogeneous, more in lymphocyte-rich areas; approximately AP/HPF (aver. 6.2/HPF) in adenocarcinoma areas [2].

J2	Heart	NHAIR
	Lung	Moderate atelectasis; moderate acute diffuse hyperaemia; focal alveolar haemorrhages. NHAIR
	Liver	Centrolobular hepatocytes contain small amount of glycogen and none is present in periportal hepatocytes. Concurrently, in one part of the section periportal cells hold modest amounts of yellow-green pigment. Similar pigment is also present in Kuppfer cells. Mild glycogen depletion
	Spleen	Section size approx. 1 x 2 mm (triangular). NHAIR
	Kidney	NHAIR
	LN	Elongated, partial section of lymphnode, approx. 3 x 1 mm. Cell-rich, cortex, paracortex, three secondary follicles; no foreign cells. CD-3: Abundant number of T cells in cortex and below cortex (DCU?) [3].
	Tumour	Elongated section, approx. 3 x 2 mm. Bordered by muscle and fibrous tissue or fibrovascular tissue. Round (2 mm) tumour filled with aggregates of MGCs and abundant calcifications (and some lucent bluish-gray material); admixed with aggregates/infiltrates of foamy ELCs; throughout sample large number of individual lymphocytes and plasma cells / loose lymphocyte infiltrates and macrophages. CD-3: Large number of T cells especially among MGC and ELC aggregates [3]. Casp-3: Less than 5 AP/HPF (aver. 2.8/HPF) among ELCs [1].

J3	Heart	NHAIR
	Lung	Marked atelectasis; moderate acute diffuse hyperaemia; focal alveolar haemorrhages. NHAIR
	Liver	A haemorrhage and a tear. Centrolobular hepatocytes contain small amount of glycogen and very little is present in periportal hepatocytes. Glycogen depletion, moderate.
	Spleen	Section size approx. 1 x 7 mm. Mildly increased numbers of heterophils in marginal zones.
	Kidney	NHAIR
	LN	T-shaped, partial section of lymphnode, approx. 3 x 1 mm. Paracortex, and medulla, cortex poorly discernible; no foreign cells. CD-3: T cells in paracortex (DCUs?) and in cortex, few in medulla [2].

J3	Tumour	Elongated section, approx. 3 x 2 mm. Bordered by muscle and fibrovascular tissue or fibrous capsule. Oval tumour filled with aggregates of MGCs and abundant calcifications (and some lucent bluish-gray material); admixed with aggregates/infiltrates of foamy ELCs; throughout sample large number of individual lymphocytes and plasma cells / loose lymphocyte infiltrates and macrophages; peripherally large infiltrates of heterophils, lymphocytes and plasma cells. CD-3: Large number of T cells especially among MGC and ELC aggregates (Peripheral infiltrates contain relatively few T cells) [3]. Casp-3: Less than 5 AP/HPF (aver. 1.4/HPF) among ELCs [1].

J4	Heart	NHAIR
	Lung	Moderate to marked atelectasis; moderate acute diffuse hyperaemia. NHAIR
	Liver	A haemorrhage and a tear. Cytoplasmic hyaline inclusions. NHAIR
	Spleen	Section size approx. 1 x 2 mm. NHAIR
	Kidney	NHAIR
	LN	Bean-shaped section of a lymph node, approx. 2 x 1 mm. Cell-rich, all parts present; 2-3 secondary follicles?; no foreign cells. CD-3: Sparse population of T cells below cortex in cortex [1].
	Tumour	Triangular section, approx. 2 mm. Without natural borders. Apex of triangle consists of fibrous tissue; in base a mixture of calcified areas and aggregates/infiltrates of foamy ELCs; some MGCs (some with lucent bluish-gray material); abundant number of individual lymphocytes and plasma cells / loose lymphocyte infiltrates and macrophages. CD-3: Large number of T cells especially among ELC aggregates and around calcified foci [3]. Casp-3: Less than 5 AP/HPF (aver. 1.6/HPF) among ELCs [1].

J5	Heart	NHAIR
	Lung	Moderate atelectasis; moderate acute diffuse hyperaemia. NHAIR
	Liver	NHAIR
	Spleen	Section size approx. 2 x 5 mm. NHAIR
	Kidney	NHAIR
	LN	Round section, approx. 2 mm. Cell-rich, cortex, paracortex, one secondary follicle; no foreign cells. CD-3: Dense population of T cells in below cortex (a DCU?) [3].
	Tumour	Oval section, approx. 2 x 1 mm. Bordered by fibrovascular tissue (with nerve fibres or fibrous capsule. Large calcified areas and several MGCs, some with lucent bluish-gray material or bright yellow granules; small number of foamy ELCs; dense infiltrates of lymphocytes and plasma cells; macrophages in periphery. CD-3: Large number of T cells diffusely outside calcified areas [4]. Casp-3: Little tissue outside necrotic areas; less than 5 AP/HPF (aver. 1.7/HPF, three fields evaluated) among ELCs [1].

J6	Heart	NHAIR
	Lung	Moderate to marked atelectasis; moderate acute diffuse hyperaemia. NHAIR
	Liver	Reduced amount of glycogen in hepatocytes. One small portal aggregate of heterophils. Minimal glycogen depletion.
	Spleen	Section size approx. 2 x 3 mm); partly broken. Minimally increased numbers of heterophils in loose aggregates in the red pulp. Lymphocyte hyperplasia, minimal.
	Kidney	NHAIR
	LN	Oval section, approx. 2 mm. Cell-rich, cortex, paracortex, two secondary follicles; no foreign cells. CD-3: Dense population of T cells in paracortex and in interfollicular cortex [3].
	Tumour	Oval section, approx. 3 x 3 mm. Bordered by partly by muscle, mostly by thin fibrous capsule. Large calcified areas and several MGCs, some with lucent bluish-gray material; admixed with foamy ELCs; abundant infiltration of lymphocytes, plasma cells and macrophages; dense infiltrates in the periphery. CD-3: Large number of T cells diffusely and in peripheral infiltrates [3]-[4]. Casp-3: Little tissue outside necrotic areas; less than 5 AP/HPF (aver. 3.7/HPF, three fields evaluated) among ELCs [1].

J7	Heart	NHAIR
	Lung	Moderate to marked atelectasis; moderate acute diffuse hyperaemia. NHAIR
	Liver	A haemorrhage and a tear. One small portal lymphocytic infiltrate.
	Spleen	Section size approx. 1 x 2 mm. NHAIR
	Kidney	NHAIR
	LN	Elongated section, approx. 2 x 1 mm. Cell-rich, medulla; paracortex; cortex, primary follicles; no foreign cells. CD-3: Dense population of T cells in paracortex and in interfollicular cortex [3].
	Tumour	Round section, approx. 1 mm. Without natural borders. Aggregates/infiltrates of foamy ELCs (some contain bright yellow granular pigment) admixed with some small calcifications and few MGCs; large number of individual lymphocytes and plasma cells / loose lymphocyte infiltrates and macrophages. CD-3: Large number of T cells individually and in aggregates [3]. Casp-3: Small section; less than 5 AP/HPF (aver. 1.3/HPF, four fields evaluated) among ELCs [1].

Fig. S1

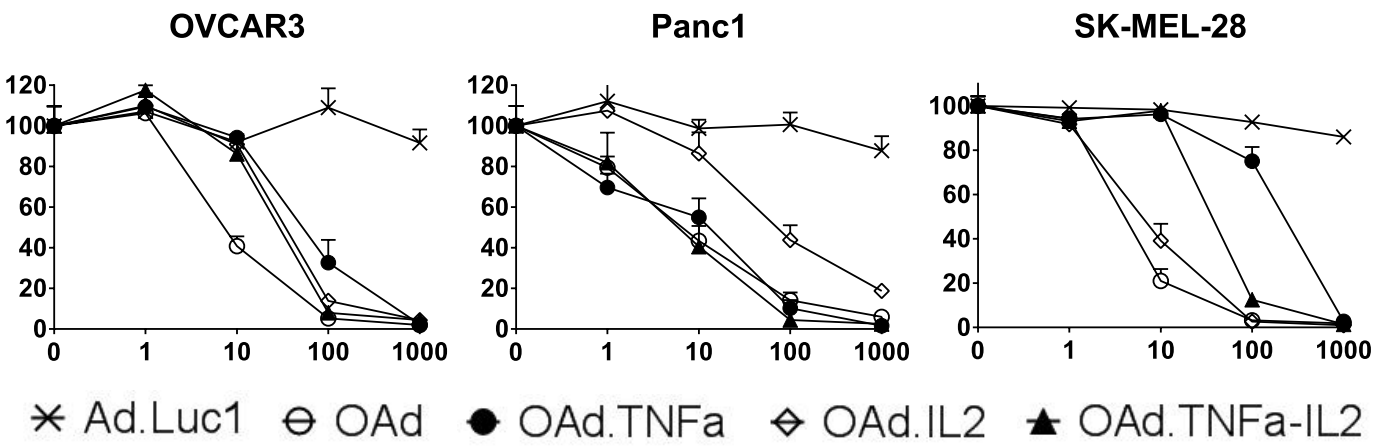

Supplementary Figure S1. Oncolytic activity of the virus in a selection of human cancer cell lines. The viruses showed oncolytic potential in ovarian cancer (OVCAR3), pancreatic cancer (Panc1), and melanoma (SK-MEL-28). The cells were incubated with viruses for four (OVCAR3 and Panc1) or six days (SK-MEL-28). Ad.Luc1 = Replication deficient Ad5/3-Luc1, OAd = Ad5/3-E2F-d24, OAd.TNFa = Ad5/3-E2F-d24-hTNFa, OAd.IL2 = Ad5/3-E2F-d24-hIL2, OAd.TNFa-IL2 = Ad5/3-E2F-d24-hTNFa-IRES-hIL2. Mean plus SD is shown.

Fig. S2

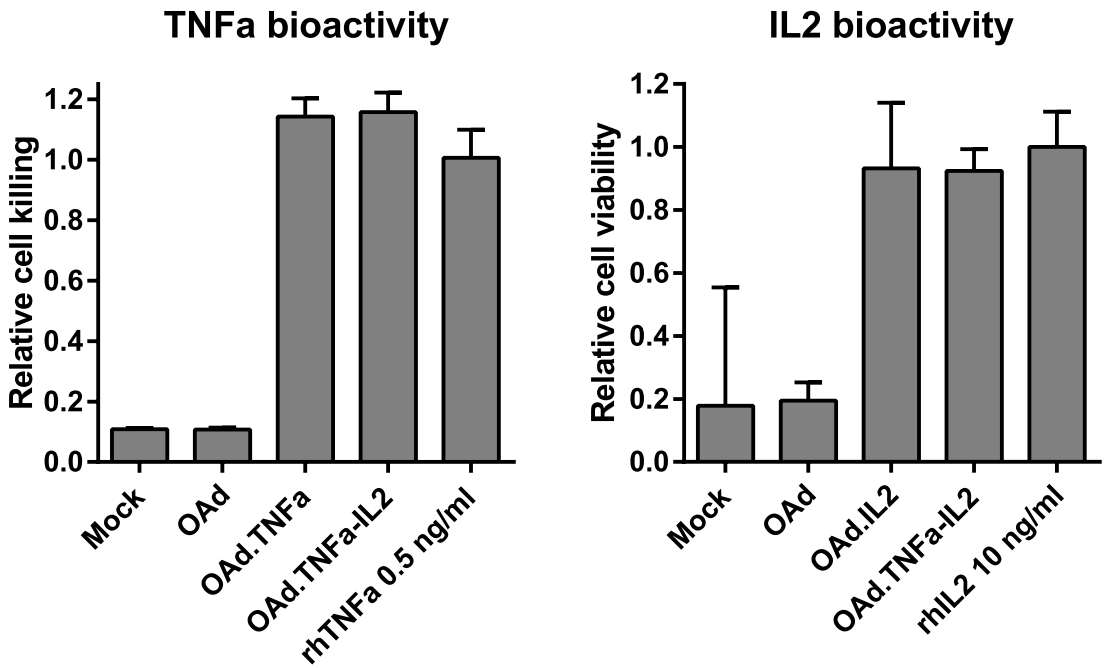

Supplementary Figure S2. Human cell lines produce biologically active cytokines when infected with armed viruses. A549 cells were infected with 1000 VP per cell for 72 hours. The supernatant was filtered and applied on indicator cell lines. TNFa-induced killing of L929 cells or IL-2-induced proliferation of CTLL-2 T cells were studied with MTS. OAd = Ad5/3-E2F-d24, OAd.TNFa = Ad5/3-E2F-d24-hTNFa, OAd.IL2 = Ad5/3-E2F-d24-hIL2, OAd.TNFa-IL2 = Ad5/3-E2F-d24-hTNFa-IRES-hIL2. Mean plus SD is shown.

Fig. S3

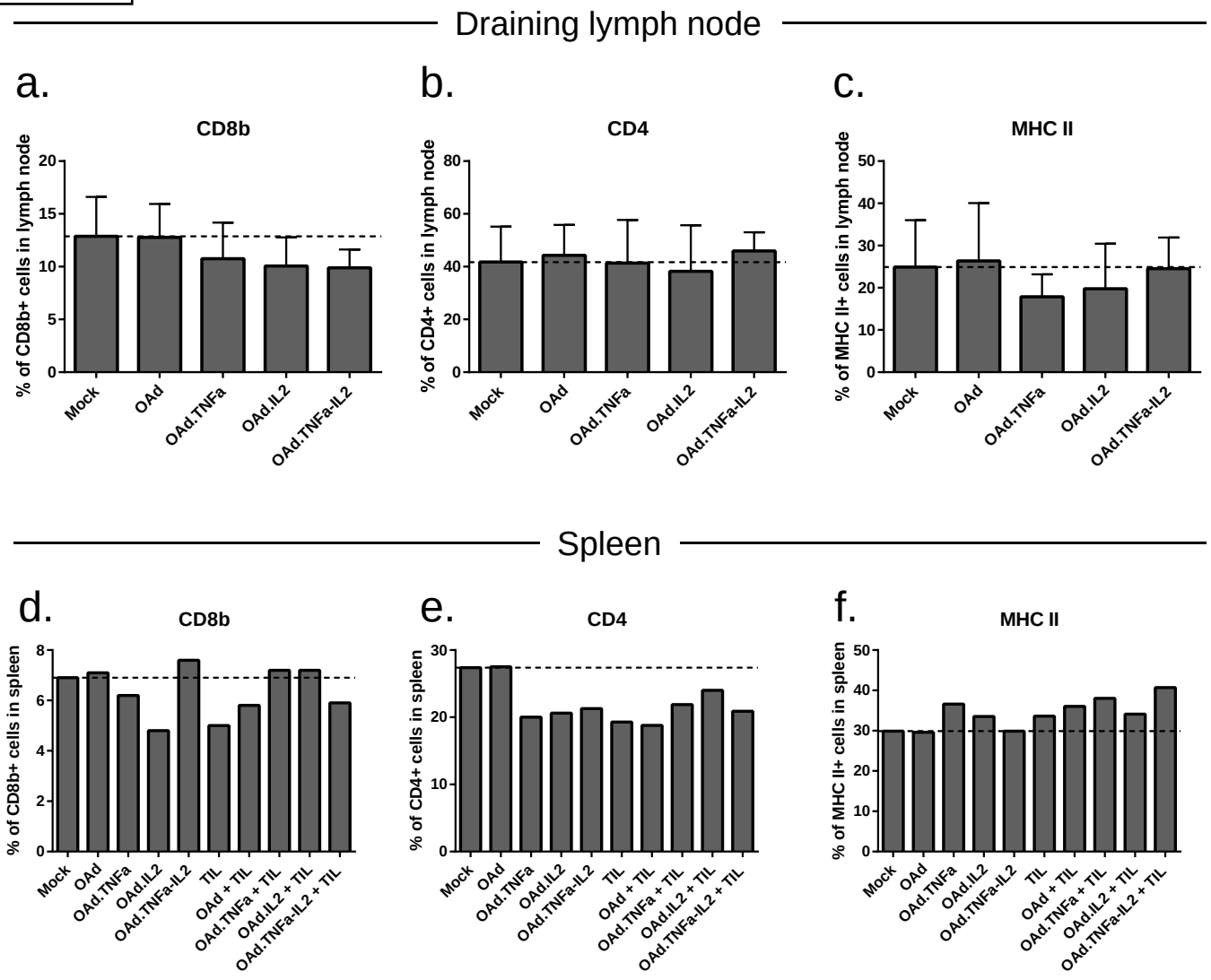

Supplementary Figure S3. Changes in immune cell subsets in tumor-draining lymph nodes and spleens. Percentage of (a) CD8+ (b) CD4+ and (c) MHC II+ cells in lymph nodes and (d–f) in pooled spleens, respectively. OAd = Ad5/3-E2F-d24, OAd.TNFa = Ad5/3-E2F-d24-hTNFa, OAd.IL2 = Ad5/3-E2F-d24-hIL2, OAd.TNFa-IL2 = Ad5/3-E2F-d24-hTNFa-IRES-hIL2. Mean plus SD is shown.